
RESOURCE-EFFICIENT FEDERATED LEARNING

Ahmed M. Abdelmoniem¹ Atal Narayan Sahu¹ Marco Canini¹ Suhaib A. Fahmy¹

ABSTRACT

Federated Learning (FL) enables distributed training by learners using local data, thereby enhancing privacy and reducing communication. However, it presents numerous challenges relating to the heterogeneity of the data distribution, device capabilities, and participant availability as deployments scale, which can impact both model convergence and bias. Existing FL schemes use random participant selection to improve fairness; however, this can result in inefficient use of resources and lower quality training. In this work, we systematically address the question of resource efficiency in FL, showing the benefits of intelligent participant selection, and incorporation of updates from straggling participants. We demonstrate how these factors enable resource efficiency while also improving trained model quality.

1 INTRODUCTION

Recently distributed machine learning (ML) deployments have sought to push computation towards data sources in an effort to enhance privacy and security (Bonawitz et al., 2019; Kairouz et al., 2019). Training models using this approach is known as Federated Learning (FL). FL presents a variety of challenges due to the high heterogeneity of participating devices, ranging from powerful edge clusters and smartphones to low-resource IoT devices (e.g., surveillance cameras, sensors, etc.). These devices produce and store the application data used to locally train a central ML model. FL is deployed by large service providers such as Apple, Google, and Facebook to train computer vision (CV) and natural language processing (NLP) models in applications such as image classification, object detection, and recommendation systems (tensorflow.org, 2020; Yang et al., 2018b; FedAI, 2021; FaceBook, 2021; Team, 2017; Hsu et al., 2020; Hartmann et al., 2019). FL has also been deployed to train models on distributed medical imaging data (Li et al., 2019); smart camera images (Jiang et al., 2019a), and live network traffic data (Yan et al., 2020). The life-cycle of FL is as follows. First, the FL developer builds the model architecture and determines hyper-parameters with a standalone dataset. The model’s training is then conducted on participating learners for a number of centrally managed rounds until satisfactory model quality is obtained. The main challenge in FL is the heterogeneity in terms of computational capability and data distribution among a large number of learners which can impact the performance of training (Bonawitz et al., 2019; Kairouz et al., 2019).

Time-to-accuracy is a crucial performance metric and is the focus of much work in this area (Lai et al., 2021b; Yang et al., 2020; Abdelmoniem & Canini, 2021b; Abdelmoniem et al., 2021a). It depends on both the statistical efficiency and system efficiency of training. The number of learners, minibatch size, local steps affect the former. It is common for these factors to be treated as hyper-parameters to be tuned for a particular FL job. System efficiency is primarily regulated by the time to complete a training round, which depends on which learners are selected and whether they become stragglers whose updates do not complete in time. It is common to configure a reporting deadline to cap the round duration, but if an insufficient number of learners complete before this deadline, the entire round fails and is re-attempted from scratch. Since a tight deadline can yield more failed rounds, this can be mitigated by overcommitting the number of selected learners in each round to increase the likelihood that a sufficient number will finish by the deadline. Failed rounds and overcommitted participants lead to wasted computation, which has mostly been ignored in previous FL approaches. A focus on time has also resulted in schemes that are not robust to non-I.I.D. data distributions due to favoring certain learner profiles. Finally, learners also have varying availability for training (Kairouz et al., 2019; Bonawitz et al., 2019; Li et al., 2021; Yang et al., 2020) which can be problematic with heterogeneous data distributions. Therefore, a practical FL system should also consider participant availability while reducing resource wastage.

We argue that resource wastage deters users from participating in FL and makes the scaling of FL systems to larger numbers and more varied computational capabilities of learners problematic. We aim to optimize the design of FL systems for their resource-to-accuracy in a heterogeneous setting. This means the computational resources consumed to reach

¹KAUST. Correspondence to: Ahmed M. Abdelmoniem <ahmed.sayed@kaust.edu.sa>.

a target accuracy should be reduced without a significant impact on time-to-accuracy. By considering heterogeneity at the heart of our design, we also intend to demonstrate improved robustness to realistic data distributions among learners.

Existing efforts aim to improve convergence speed (i.e., boosting model quality in fewer rounds) (Li et al., 2020a; Wang & Joshi, 2019) or system efficiency (i.e., reducing round duration) (McMahan et al., 2017; 2018), or selecting learners with high statistical and system utility (Lai et al., 2021b). These systems ignore the importance of maximizing the utilization of available resources while reducing the amount of wasted work. To address these problems, we introduce *RELAY*, a practical scheme that maximizes existing FL systems’ statistical, system, and resource efficiency. *RELAY* accomplishes this by decoupling the collection of participant updates from aggregation into an updated model. *RELAY* also intelligently selects among available participants that are least likely to be available in the future. *RELAY* achieves this with little modification to the existing FL solutions (Bonawitz et al., 2019; Lai et al., 2021b).

We summarize our contributions in this paper:

1. We highlight the importance of efficient resource usage in FL due to the limited capability and availability of edge devices and present *RELAY* to intelligently select participants and efficiently make use of their resources.
2. We propose staleness-aware aggregation and intelligent participant selection algorithms to improve resource usage with minimal impact on time-to-accuracy.
3. We implement and evaluate *RELAY* using a wide-range of real-world FL benchmarks and compare it with the state-of-the-art to show the significant benefits it can bring to existing FL systems.

2 BACKGROUND

We review the FL ecosystem with a focus on system design considerations, highlighting major challenges based on empirical evidence from real datasets. We motivate our work by highlighting the main drawbacks of existing designs.

2.1 Federated Learning

We consider the popular FL setting introduced in federated averaging (FedAvg) (McMahan et al., 2017; Bonawitz et al., 2019). The FedAvg model consists of a (logically) centralized server and distributed learners, such as smartphones or IoT devices. Learners locally maintain private data and collaboratively train a joint global model. A key assumption in FL is a lack of trust, implying training data should not leave the data source (Bonawitz et al., 2017), and any possible breach of private data during communication should be avoided (Bonawitz et al., 2019; Kairouz et al., 2019).

The training of the global model is conducted over a series of rounds. As shown in Fig. 1, at the beginning of each training round, the server waits (during a selection window)

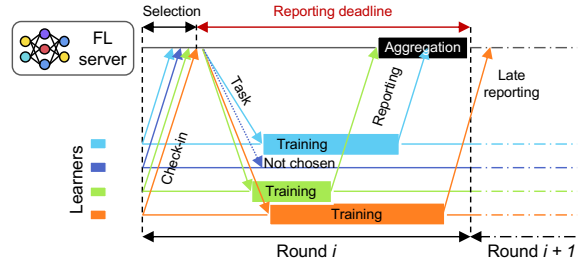


Figure 1: A round of training in FL. A sample of learners, called participants, perform training in a given round.

for a sufficient number of available learners to check-in.¹ Then, the server samples a subset of the checked-in learners – called participants – to train in the current round. The participants fetch the latest version of the model along with any necessary configurations (e.g., hyper-parameter settings). Each participant trains the model on its local data for a specified number of epochs and produces a model update (i.e., the delta from the global model) which it sends to the server. The server waits until a target number of participants send their updates to aggregate them and update the global model. This concludes the current round and the former steps are repeated in each round until a certain objective is met (e.g., target model quality or training budget).

To ensure progress, the server generally waits for model updates until a reporting deadline. Updates from stragglers that may arrive beyond the deadline are discarded. A round is considered successful if at least a target number of participants’ updates are received by the deadline, else the round is aborted and a new one is attempted.

The FL setting is also distinct from conventional ML training because the distributed learners may exhibit the following types of heterogeneity: 1) **data heterogeneity**: learners generally possess variable data points in number, type, and distribution; 2) **device heterogeneity**: learner devices have different speeds owing to different hardware and network capabilities; 3) **behavioral heterogeneity**: the availability of learners varies across rounds and there may be learners that abandon the current round if they become unavailable. Heterogeneity creates several challenges for FL system designers because both the quality of the trained model and the training speed are majorly affected by which participants are selected at each round. Below we briefly review existing designs that serve as context to motivate our distinct approach (§3). We discuss additional related work in §6.

2.2 Existing FL Systems

Accounting for the unreliability and heterogeneity of learners, SAFA (Wu et al., 2021) enables semi-asynchronous updates from straggling participants.

¹A learner is considered available if it meets certain participation conditions: typically, being connected to power, being idle, and using an unmetered network (Bonawitz et al., 2019).

SAFA flips the participant selection process of FedAvg: it runs training on *all* learners and ends a round when a pre-set percentage of them return their updates. SAFA allows participants to report after the round deadline, in which case the updates are cached and applied in a later round. However, SAFA only tolerates updates from learners that are within a bounded staleness threshold. Therefore, the round duration in SAFA is reduced by only waiting for a fraction of the participants, while the cache ensures that the computational effort of straggling participants is not entirely wasted and is able to boost statistical efficiency. FLEET (Damaskinos et al., 2020) also enables stale updates but adopts a dampening factor to give smaller weight as staleness increases. This has the advantage of not discarding updates that exceed the staleness threshold. However, their AdaSGD protocol is not directly compatible with the traditional FL settings such as FedAvg and FLEET synchronizes model gradients after every single local mini-batch.

Oort (Lai et al., 2021b) uses a participant selection algorithm that favors learners with higher utility. The utility of a learner in Oort is comprised of statistical and system utility. The statistical utility is measured using training loss as a proxy while system utility is measured as a function of completion time. Oort preferentially selects fast learners to reduce the round duration. At the same time, it uses a pacer algorithm that can trade longer round duration to include unexplored (or slow) learners when required for statistical efficiency.

3 CASE FOR RESOURCE-EFFICIENT FL

We motivate *RELAY* by highlighting the trade-offs between system efficiency and resource diversity as conflicting optimization goals in FL. Navigating the extremes of these two objectives, as exhibited by the aforementioned state-of-the-art FL systems, we show empirically how they fall short on common FL benchmarks.

3.1 System Efficiency vs. Resource Diversity

Current FL designs either aim at reducing the time-to-accuracy (i.e., system efficiency) (Lai et al., 2021b) or increasing coverage of the pool of learners to enhance the data distributions and fairly spread the training workload (i.e., resource diversity) (Xie et al., 2019; Li et al., 2020a; Wu et al., 2021). The former goal results in a discriminatory approach towards certain categories of learners, either preferentially selecting computationally fast learners or learners with model updates of high quality (i.e., those with high statistical utility) (Li et al., 2020a; Lai et al., 2021b). The latter goal entails spreading out the computations ideally over all available learners but at the cost of potentially longer round duration (Xie et al., 2019; Wu et al., 2021).

These two conflicting goals present a challenging trade-off for designers of FL systems to navigate. On one side of the extreme, as adopted by Oort, the designer can aggres-

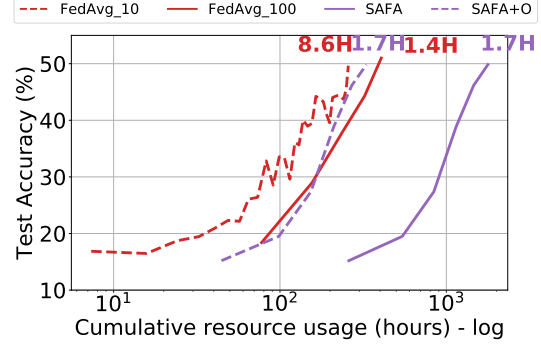


Figure 2: Performance comparison of SAFA and its resource optimized version denoted as SAFA+O.

sively optimize system efficiency and ignore the diversity of learners’ data in order to improve time-to-accuracy. The implication of this extreme is a less robust model towards high levels of data heterogeneity and consequently a model with low-levels of fairness towards the majority of the learners. On the other hand, as in SAFA, the designer could forego pre-training selection and select all available learners to maximize resource diversity.

To strike a balance between the two extremes, the FL designer would prefer a sufficient level of resource diversity without sacrificing significantly in terms of system efficiency. Our goal is to synthesize the opportunities presented by existing systems and devise a new holistic approach that can fulfill the resource diversity and system efficiency goals simultaneously, thereby addressing this trade-off. We first show that the existing systems fail to achieve both of these goals and result in significant wastage of resources. We also highlight the opportunities they present which we embrace in our design of *RELAY*.

3.2 Stale Updates & Resource Wastage

Taking inspiration from asynchronous methods (Ho et al., 2013; Xie et al., 2019), SAFA allows straggling participants to contribute to the global model via stale updates. We first evaluate SAFA’s resource usage (i.e., the time cumulatively spent by learners in training), and resource wastage (i.e., the time cumulatively spent by learners producing updates that are *not* incorporated into the model). We compare the performance of SAFA as described in (Wu et al., 2021) against a version (called SAFA+O) which assumes a perfect oracle that knows which stale updates are eventually aggregated (i.e., will not exceed the staleness threshold). We set the staleness threshold to 5 rounds and the target participant percentage to 10%. We use the Google Speech benchmark with FedScale’s data-to-learner mapping (c.f. Table 1 for details). We set the total number of learners to 1,000, and the round deadline to 100s. We use a real-world user behavior trace to induce learner’s availability dynamics (Yang et al., 2020).

Fig. 2 shows the resource usage (x-axis) and resulting test accuracy (y-axis); the lines are annotated with the time to achieve the final accuracy. Since the round time is bounded

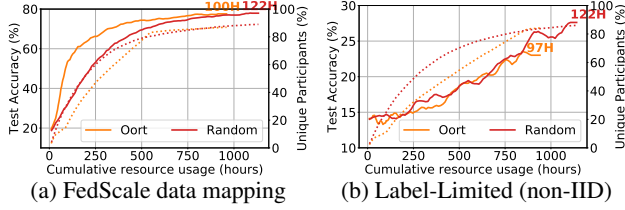


Figure 3: Impact of data heterogeneity.

by a deadline, both SAFA and SAFA+O have equal run times. Notably, SAFA is inefficient in terms of resource usage, consuming nearly $5\times$ the resources of SAFA+O to achieve the same final accuracy. By selecting all available learners, then eventually discarding a large number of the computed updates, SAFA wastes around 80% of learners’ computation time. The plot also includes runs of FedAvg with Random selection of 10 and 100 participants. Despite having low resource wastage, FedAvg with 10 participants incurs significantly higher run-time (5X) to reach the same accuracy of SAFA; the resource usage could be traded for lower run-time with 100 participants, to achieve the same accuracy at a resource usage than SAFA+O. (Uniform random data mapping yields similar results.)

Opportunity. In principle, allowing stale updates enables a reduction in round duration and achieves better time-to-accuracy while preserving the contribution of stragglers. The main challenge is, however, to balance the number of participants to avoid significant resource wastage. But balancing participant is in turn difficult because the system must estimate the on-device training time and reason about the probability of learners dropping out or exceeding the staleness threshold. This suggests that beyond stale updates, we need to tackle resource diversity directly.

3.3 Participant Selection & Resource Diversity

Many existing FL systems select participants using a uniform random sampler (Caldas et al., 2018; Yang et al., 2018b; Bonawitz et al., 2019). As noted in Oort (Lai et al., 2021b), this simple strategy is prone to select learners with disparate compute capabilities and prolong round duration due to stragglers. On the other hand, Oort’s approach of selecting fast learners has unfavorable consequences, by biasing the model to a subset of the learners due to lack of data diversity.

To see this in practice, we compare the Oort participant selector with a random sampler (Random). We use the Google Speech benchmark for 1,000 training rounds and compare two scenarios with different data mappings. In the first, data points are uniformly distributed among the participants and participants have samples from all labels (IID setting). In the second, data points are also uniformly distributed among the participants but each participant is constrained to have $\approx 10\%$ of all labels (non-IID setting). To emphasize the effect of the sampling strategy, we set all learners to be always available; we investigate the effects of

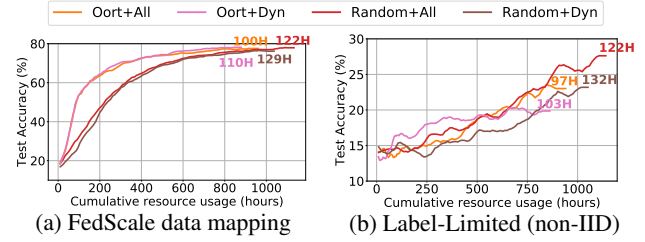


Figure 4: Impact of availability on model quality.

availability dynamics afterward.

Fig. 3 shows the test accuracy against resource usage. In the IID case, Oort is clearly superior to random selection as Oort significantly reduces the round duration by exploiting fast learners. Conversely, in the non-IID case (label-limited mapping), random selection achieves higher accuracy with a minor increase in run time due to a higher resource (and data) diversity (the right y-axis and dotted lines indicate the percentage of unique participants during training).

Participant availability impacts the global data distribution represented in the global model (Huang et al., 2021). Our analysis of a large-scale device behavior trace from Yang et al. involving more than 136K users of an FL application over a week reveals that 70% of the learners are only available for less than 10 minutes while 50% are available at least 5 minutes. This implies that in practice FL rounds should typically last a few minutes to obtain updates from the majority of participants. The analysis also suggests that low availability learners may require special consideration to increase the number of unique participants.

We now repeat similar experiments on the IID and non-IID cases of the Google Speech benchmark and contrast the execution of Random participant selection in two conditions: 1. all learners are available (AllAvail); 2. learners’ availability is dynamic according to the trace of device behavior (DynAvail). Fig. 4 reports the results. Learner availability has no tangible impact in the IID case since therein learners hold data points with comparable distributions. In the non-IID case, learners’ availability has a significant effect on accuracy (we observe a 10-point drop).

Opportunity. Generally, to have better model generalization performance, the model should be trained jointly on data samples from a large fraction of the learners’ population. While Oort’s insights into informed participant selection enable a faster round duration, there needs to be more consideration with regard to the dynamic availability of learners. This suggests that beyond learners’ diversity and compute capabilities, we need to effectively prioritize learners whose availability is limited.

4 RELAY DESIGN

RELAY’s objective is to enhance the resource efficiency of the FL training process by maximizing resource diversity without sacrificing system efficiency.

RELAY achieves this by reducing resource wastage from

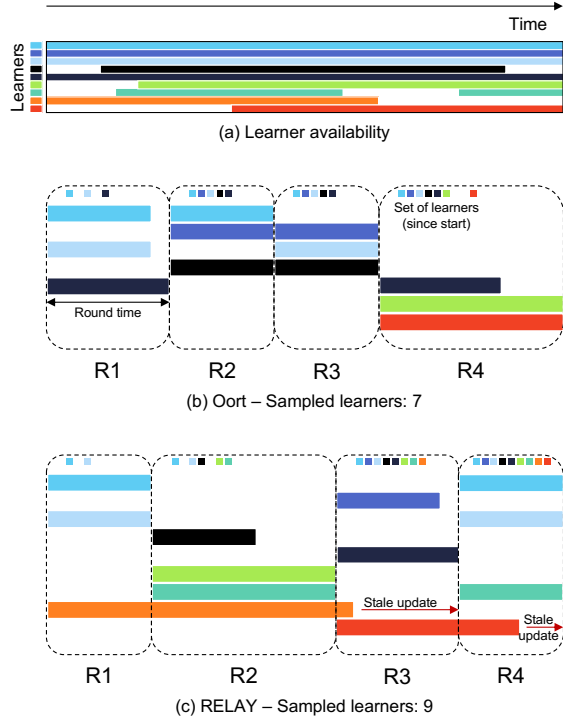


Figure 5: Example trace of 4 training rounds illustrating the main differences between Oort (b) and *RELAY* (c). The dynamic availability of 9 color-coded learners is shown in (a). By optimizing for time-to-accuracy, Oort skews participant selection towards faster learners during the early phases of training, thereby missing limited-availability learners (■ and ■). Oort’s round time is determined by stragglers. By allowing stale updates, *RELAY* lowers the dependency on stragglers. By prioritizing learners based on estimated availability, *RELAY* samples a more diverse set of learners.

delayed participants and prioritizing those with reduced availability. It leverages a theoretically-backed method to incorporate stale updates based on their quality which helps improve the training performance. It proposes a scaling rule for aggregation weights to mitigate stale updates’ impact. After an illustrative example (below), this section details the two core components of *RELAY*:

1. Intelligent Participant Selection (IPS): to prioritize participants that improve resource diversity;
2. Staleness-Aware Aggregation (SAA): to improve resource efficiency without impacting time-to-accuracy.

Overview by example. To illustrate the main differences, Fig. 5 contrasts *RELAY* with Oort. First, *RELAY* enables learners’ tracking of the availability patterns which help with predicting the future availability. Therefore *RELAY* is able to prioritize the least available participants (i.e., ■ and ■ in Fig. 5) to maximize training coverage of different learners’ data distributions. *RELAY* also allows straggling participants to submit late results beyond the set round duration (i.e., ■ and ■ in Fig. 5). Unlike Oort, which discards these updates due to their inferior device capabilities, this

Algorithm 1: Priority Selection Algorithm

Input : N_t -Target number of participants
Output : S -List of selected participants
Initialize $S_t = \Phi$, $P_t = \Phi$, $a = (\mu_t, 2\mu_t)$
On_Event *Learner_Check_In*
 Send slot a to learner l ;
 Learner l sends availability probability p_l
 $P_t = P_t \cup p_l$;
On_Event *End_Selection_Window*
 Sort in ascending order P_t ;
 Randomly shuffle P_t for probabilities with ties;
 Return S_t as the top N_t learners in P_t ;

approach reduces the wasted work of stragglers who might own valuable data for the model to be trained on.

4.1 Intelligent Participant Selection

IPS increases resource diversity to allow the global model to capture a wide distribution of learners’ data.

Adaptive Participant Target (APT): IPS can optimize the resource usage by adapting the pre-set target number of participants N_0 selected by the developer. First, the server updates its moving average estimate of round duration $\mu_t = (1 - \alpha)D_{t-1} + \alpha\mu_{t-1}$, where D_{t-1} is the duration of the previous round $t - 1$. Then, the server probes each current straggler $s \in L_s$ (from round $t - 1$) for an estimate of its expected remaining time to upload the update RT_s . Then, the server computes how many stragglers B_t can complete within the duration of the round (i.e., $RT_s \leq \mu_t$). Then, the target number of participants is adjusted for round t to $N_t = \max(1, N_0 - B_t)$.

Least Available Prioritization: Algorithm 1 describes how the IPS module intelligently selects participants from the large pool of available learners. Each learner periodically trains a model that predicts its future availability. Upon check-in of the learner l , the server sends the running average estimate of round duration μ_t . The learner uses the prediction model to determine the probability of its availability in the time slot $[\mu_t, 2\mu_t]$ and reports this to the server. At the end of the selection window, the server sorts in ascending order the learners’ probabilities P and randomly shuffles tied learners. Then, the server selects the top N_t learners to participate in this round. Similar to Google’s FL system (Bonawitz et al., 2019), the participants hold from checking-in with the server for a number of rounds (e.g., 5 rounds) after submitting their updates.

4.2 Staleness-Aware Aggregation (SAA)

This module enables the participants to submit their updates past the round deadline and processes the stale and fresh updates as described in Algorithm 2.

4.2.1 Convergence Analysis

In the following, we theoretically demonstrate that FedAvg with stale updates can converge and obtain the convergence

Algorithm 2: Stale Synchronous FedAvg

Input : K -synchronization interval, τ -delay in rounds, N_t -number of participants
Initialize $x_0 = x_1 = \dots = x_{\tau-1} \in \mathbb{R}^d$;
for Round $t = 0, \dots, T-1$ **do**
 The server samples S_t learners with $|S_t| = N_t$;
 for participant $i \in [n]$ **in parallel do**
 $y_{t,0}^i = x_t$;
 for iteration $k = 0, \dots, K-1$ **do**
 Compute a stochastic gradient $g_{t,k}^i$;
 $y_{t,k+1}^i = y_{t,k}^i - \gamma g_{t,k}^i$ /* Local participant update */;
 Let $\Delta_t^i = y_{t,K}^i - y_{t,0}^i = -\gamma \sum_{k=0}^{K-1} g_{t,k}^i$.
 Send Δ_t^i to the server;
 At Server:
 if $t < \tau$ **then**
 Broadcast x_{t+1} to participants. /* Server aggregation starts at $t = \tau$ */
 else
 Receive $\Delta_{t-\tau}^i, i \in S$; /* Update arrives with delay τ */
 Let $\Delta_{t-\tau} = \frac{1}{|S|} \sum_{i \in S} \Delta_{t-\tau}^i$;
 Server Update: $x_{t+1} = x_t + \gamma \Delta_{t-\tau}$;
 Broadcast x_{t+1} to participants.

rate. Consider the following federated optimization problem consisting of a total of m devices:

$$\min_{x \in \mathbb{R}^d} f(x) := \frac{1}{m} \sum_{j \in [m]} f_j(x), \quad (1)$$

where $f_i(x) = \mathbb{E}_{z_i \sim \mathcal{D}} l(x; z_i)$ denotes the loss function evaluated on input z_i sampled from \mathcal{D} . Algorithm 2 gives the pseudo-code of Stale Synchronous FedAvg to solve (1). Here, $g_{t,k}^i$ denotes the stochastic gradient computed at the participant corresponding to the i^{th} index at round t , and at local iteration k , such that $g_{t,k}^i = \nabla f(y_{t,k}^i) + \xi_{t,k}^i$ with $\mathbb{E}[\xi_{t,k}^i | x_{t,k}^i] = \mathbf{0}$.

For ease of exposition, we have considered a fixed τ round delay in Algorithm 2. However, our analysis holds for variable delays bounded by τ .

4.2.2 Assumptions

We consider the following general assumptions on the loss function.

Assumption 1. (Smoothness) The function, $f_i : \mathbb{R}^d \rightarrow \mathbb{R}$ at each participant, $i \in [n]$ is L -smooth, i.e., for every $x, y \in \mathbb{R}^d$ we have, $f_i(y) \leq f_i(x) + \langle \nabla f_i(x), y - x \rangle + \frac{L}{2} \|y - x\|^2$.

Assumption 2. (Global minimum) There exists x_* such that, $f(x_*) = f^* \leq f(x)$, for all $x \in \mathbb{R}^d$.

Assumption 3. ((M, σ^2) bounded noise) (Stich & Karimireddy, 2020) For every stochastic noise $\xi_{t,k}^i$, there exist $M \geq 0, \sigma^2 > 0$, such that $\mathbb{E}[\|\xi_{t,k}^i\|^2 | x_t] \leq M \|\nabla f(x_{t,k}^i)\|^2 + \sigma^2$, for all $x_t \in \mathbb{R}^d$.

4.2.3 Convergence result

The next theorem provides the non-convex convergence rate.

Theorem 1. Let Assumptions 1, 2, and 3 hold. Then, for Algorithm 2, we have

$$\frac{1}{nTK} \sum_{t=0}^{T-1} \sum_{i=1}^n \sum_{k=0}^{K-1} \mathbb{E} \|\nabla f(y_{t,k}^i)\|^2 = \mathcal{O} \left(\frac{\sigma \sqrt{L(f(x_0) - f^*)}}{\sqrt{nTK}} + \frac{\max\{L\sqrt{\tau K(n\tau K + M)}, L(K + M/n)\}}{TK} \right).$$

In §B, we give detailed proofs of the convergence analysis. We achieve a $\mathcal{O}(\frac{1}{\sqrt{nTK}})$ asymptotic rate, which improves with K , the number of local steps per round. In comparison, the Asynchronous algorithm of (Xie et al., 2019) does not improve with the number of local steps. Moreover, asynchrony (captured by τ) only affects the faster decaying $\mathcal{O}(\frac{1}{T})$ term. Thus, Stale Synchronous FedAvg has the same asymptotic convergence rate as synchronous FedAvg (Stich & Karimireddy, 2020), and hence achieves asynchrony for free. Furthermore, this asymptotic rate will be better for Stale Synchronous FedAvg in practice, since the rate improves with n , the total number of learners contributing to an update, and staleness relaxation should result in more learners contributing to an update. We note that our convergence guarantee depends on the maximum round delay τ , and large round delays could impact the convergence, and therefore this impact should be mitigated.

4.2.4 Mitigating the Impact of Large Staleness

To mitigate the impact, prior work on distributed asynchronous training proposes to scale the weight of stale updates before aggregation (Zhang et al., 2016; Jiang et al., 2017; Damaskinos et al., 2020). We denote the set of fresh and stale updates in a round as \mathcal{F} , and \mathcal{S} respectively. Let $n_{\mathcal{F}}$ be the number of fresh updates, and $\hat{u}_{\mathcal{F}}$ be the average of the fresh updates. Moreover, let $n_{\mathcal{S}}$ be the number of stale updates, and for a straggler $s \in \mathcal{S}$, u_s be the stale update, and τ_s be the number of rounds the straggler is delayed by. The following are the scaling rules in the literature:

1. **Equal:** same weight as fresh updates (i.e., $w_s = 1$).
2. **DynSGD:** linear inverse of the number of staleness rounds $w_s = \frac{1}{\tau_s + 1}$ (Jiang et al., 2017).
3. **AdaSGD:** exponential damping of the number of staleness rounds $w_s = e^{-(\tau_s + 1)}$ (Damaskinos et al., 2020).

(Damaskinos et al., 2020) also proposed a boosting multiplier to increase the weights for stale updates to account for learners with data distributions largely variable from the global data distribution. They show that boosting the weight of important stale updates is critical since stragglers may possess more valuable (dissimilar) data distribution as compared to fast learners. However, this approach may violate privacy because to compute the boosting factor, the learners need to share information about their data.

Therefore in this work, we propose a privacy-preserving

boosting factor and combine it with the staleness-based damping rule of DynSGD (Jiang et al., 2017). The proposed boosting factor favors a stale update based on how much it deviates from the fresh updates’ average and hence it does not require any information about learner’s data. Let, $\Lambda_s = \frac{\|\hat{u}_{\mathcal{F}} - \frac{u_s + n_{\mathcal{F}} \hat{u}_{\mathcal{F}}}{n_{\mathcal{F}} + 1}\|^2}{\|\hat{u}_{\mathcal{F}}\|^2}$ be the deviation of the stale update u_s from the average of the fresh updates $\hat{u}_{\mathcal{F}}$. Let $\Lambda_{max} = \max_{s \in \mathcal{S}} \Lambda_s$. The boosting factor term scales a stale update s proportional to $1 - e^{-\frac{\Lambda_s}{\Lambda_{max}}}$. Finally, our rule to compute the scaling factor is:

$$w_s = (1 - \beta) \frac{1}{\tau_s + 1} + \beta(1 - e^{-\frac{\Lambda_s}{\Lambda_{max}}}) \quad (2)$$

where β is a tunable weight for the averaging.

For every fresh update $f \in \mathcal{F}$, we choose a scale value of one, i.e. $w_f = 1$. The final coefficients for weighted averaging are the normalized weights. That is, for an update $i \in \mathcal{F} \cup \mathcal{S}$, the final coefficient $\hat{w}_i = \frac{w_i}{\sum_{i \in \mathcal{F} \cup \mathcal{S}} w_i}$.

5 EVALUATION

We evaluate *RELAY* by answering the following questions: 1) Is prioritizing learners based on availability beneficial? 2) Does aggregation of stale updates reduce resource usage and improve model quality? 3) Should stale updates be weighted differently to fresh updates? 4) Is *RELAY* scalable and future-proof?

We summarize the main observations as follows:

1. Over several benchmarks and experimental settings, *RELAY* achieves better model quality with up to $2\times$ resource savings compared to existing systems.
2. *RELAY* results in quality gains in different scenarios involving both IID and non-IID data distributions.
3. The proposed weight scaling can boost the statistical efficiency of *RELAY*.
4. *RELAY* scales well and is more robust to future hardware advancements than other schemes.

5.1 Experimental Setup

Our experiments simulate FL benchmarks consisting of learners using real-world device configurations and availability traces. We use a Nvidia GPU cluster to interleave the training of the simulated learners. The round participants train in parallel on time-multiplexed GPUs (i.e., 2-4 GPUs per run) using PyTorch v1.8.0.

Benchmarks: We experiment with the benchmarks listed in Table 1, that span several common FL tasks of different scales to cover varied practical scenarios. The datasets consist of hundreds or up to millions of data samples (c.f. §E for datasets description). By default, FedAvg (McMahan et al., 2017) is used as the aggregation algorithm for the CIFAR10 benchmark and YoGi (Ramaswamy et al., 2020) for other benchmarks similar to (Lai et al., 2021b).

Data Partitioning: The FedScale data to learner mappings encompass thousands to millions of learners (Lai et al.,

2021a) (see §E.1). For the Google Speech benchmark, we observe that most labels appear at least once on more than 40% of the learners, making this close to a full uniform (IID) distribution, simplifying training. The same observations are made for the other benchmarks. We introduce more realistic heterogeneous data mappings. We partition the training dataset among the learners using different methods, from easy to hard: D1) **Random uniform mapping (IID)**: a uniform distribution among all learners; D2) **FedScale data to learner mappings**: as in (Lai et al., 2021a) in which the data distribution reflects real data sources;² D3) **Label-limited mapping**: learners assigned data samples drawn from a random subset of labels as listed in Table 1, with data samples per learner following particular distributions as follows: L1) **balanced distribution**: using an equal number of samples for each data label on each learner; L2) **uniform distribution**: using uniform random assignment of data points to labels on each learner; L3) **Zipf distribution**: Zipfian distribution with $\alpha = 1.95$ to have higher level of label skew (popularity).

System Performance of Learners: Learners’ hardware performance is assigned at random from profiles of real device measurements from the AI (Benchmark, 2021) and MobiPerf (M-Lab, 2021) benchmarks for inference time and network speeds of mobile devices, respectively. (We show how the distribution of floating-point and quantized inference time from the AI benchmark and device profiles can clustered into 6 different device configurations demonstrating significant device heterogeneity in §C). The profiles represent devices with at least 2GB RAM using WiFi which matches the common practice in FL settings (Yang et al., 2018b; Bonawitz et al., 2019; Lai et al., 2021b).

Availability Dynamics of Learners: We use a trace of 136k mobile users from different countries over a period of 1-week (Yang et al., 2020). The trace contains ≈ 180 million entries for events such as connecting to WiFi, charging the battery, and (un)locking the screen, etc. Availability is defined as when a device is connected to a charger, similar to (tensorflow.org, 2020; Lai et al., 2021b). In §C we demonstrate that learners exhibit diurnal variations (and cyclic behavior) and the majority of the learners stay available for only a few minutes.

RELAY setup: unless otherwise stated, no threshold is applied on the staleness rounds of the stale updates. We set $\alpha = 0.25$ for the moving average of round duration. We set $\beta = 0.35$ for the weight scaling in Eq. (2).

Experimental Scenarios: We consider 2 experimental settings used in the literature:

1. **OC:** the FL server over-commits the target number of participants N_t by 30% and waits for the updates from the N_t participants similar to (Lai et al., 2021b;a).

²For instance, images collected from Flickr in OpenImage have a AuthorProfileUrl attribute that can be used to map data learners, though these may not reflect real data mappings in FL scenarios.

Table 1: Summary of the benchmarks used in this work.

Task	Model	Dataset	Model Size # of Parameters	Learning Rate	Local Epochs	Batch Size	FedScale Mapping			Artificial Mapping		
							# of samples	Total Learners	# of Labels	# of samples	Total Learners	# of Labels
Image Classification	ResNet18 (He et al., 2016)	CIFAR10 (Krizhevsky, 2009)	11.4Mil	0.01	1	10	50K	3K	10	50K	3K	4
	ShuffleNet (Zhang et al., 2018)	OpenImage (Kuznetsova et al., 2020)	1.4Mil	0.01	5	30	1.4Mil	15K	600	2Mil	3K	60
Speech Recognition	ResNet34 (He et al., 2016)	Google Speech (Warden, 2018)	21.5Mil	0.005	1	20	200K	3K	35	200K	3K	4
Natural Language Processing	Albert (Lan et al., 2020)	Reddit (Pushshift, 2020)	11Mil	0.0001	5	40	42Mil	16mil	10	8.4Mil	3K	N/A
		Stackoverflow (McMahan et al., 2017)	11Mil	0.0008	5	40	43mil	300K	10	8.6Mil	3K	N/A

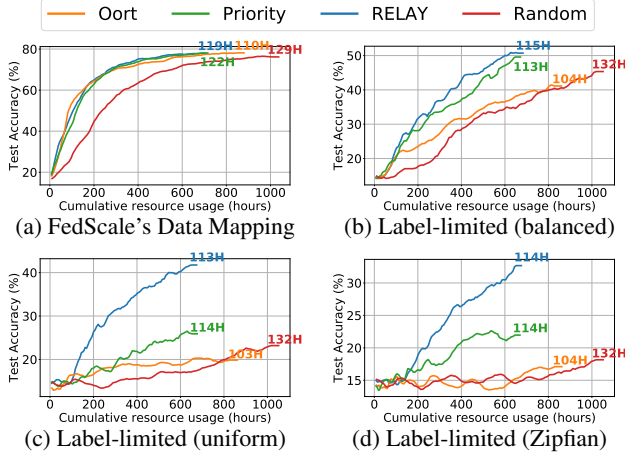


Figure 6: Training performance comparison under OC+DynAvail across different data mappings.

2. **DL**: the FL server chooses a target number of participants N_t and aggregates any number of updates received before the end of a pre-set deadline similar to (Yang et al., 2020; Bonawitz et al., 2019).

Unless otherwise mentioned, the target number of participants is 10 and each experiment is repeated 3 times with different sampling seeds and the average of the three runs is shown. The experiments use $\approx 13K$ hours of GPU time.

5.2 Experimental Results

We evaluate the amount of learner resources (and run-time) spent to achieve certain test accuracy (*the lower resources and time used are the better*).³ Here, we focus on Google Speech and present the results of other benchmarks and experimental settings in §D. For reference, in §E, we present the baseline test accuracy achieved by training the models of different benchmarks in a semi-centralized manner (i.e., data-parallel distributed learning) where the dataset is only divided among 10 learners who participate fully in every training round.

Performance of Selection Algorithms: We use the experimental setting OC+DynAvail. We compare *RELAY* with Oort, Random, and Priority selection. Priority is the IPS module of *RELAY* (i.e., SAA module is disabled). Fig. 6 shows that, over the FedScale and different non-IID (label-

³Cumulative resources is the sum of the total computational and communication time spent by the participants including those that produce updates that are not aggregated.

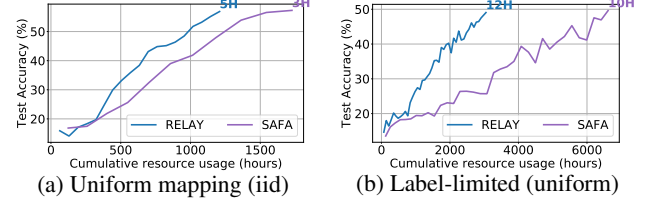


Figure 7: Comparison against SAFA.

limited) data mappings, with minimal resource usage, *RELAY* achieves better accuracy over other methods (i.e., Oort, Random, and Priority). *RELAY* achieves superior performance thanks to the availability-based prioritization (IPS module) and aggregation of stale updates (SAA module). (In §D we show results for more rounds demonstrating *RELAY* converging to significantly higher accuracy than Oort, while using fewer resources and in less time.

Performance of Aggregation Algorithms: We use DL+DynAvail to evaluate SAFA and *RELAY* with a total learner population of 1000 and a round deadline of 100s. We use FedAvg as the underlying aggregation algorithm. *RELAY* pre-selects 100 participants and the target ratio is set to 10% and 80% for SAFA and *RELAY*, respectively. For both schemes, we set the staleness threshold to 5 rounds. The results in Fig. 7 show that run-times of SAFA and *RELAY* are comparable, but SAFA consumes significantly more resources. In the case of the FedScale mapping (Fig. 7a), the results show that *RELAY* achieves higher accuracy with $\approx 20\%$ fewer resources than SAFA. In the non-IID mapping (Fig. 7b), *RELAY* significantly improves the accuracy by 10 points using $\approx 60\%$ fewer resources compared to SAFA. Next, we evaluate the availability-based prioritization, stale aggregation, and weight scaling techniques of *RELAY*.

Availability Prioritization: The results in Fig. 6 show that Priority selection achieves better model accuracy thanks to prioritizing the least available learners. The results suggest that, especially in non-IID settings, selecting participants with low availability results in a better rate of unique learners with valuable (likely new) data samples, and hence the resource usage to achieve a certain accuracy is also reduced.

Adaptive Target: We run experiments in OC setting with both DynAvail and AllAvail scenarios using the label-limited (uniform) mapping and 50 participants per round. Fig. 8 shows, in both scenarios, *RELAY* and *RELAY* +APT have higher model quality with lower resources compared to Oort and Random. Moreover, by trading off extra run-time,

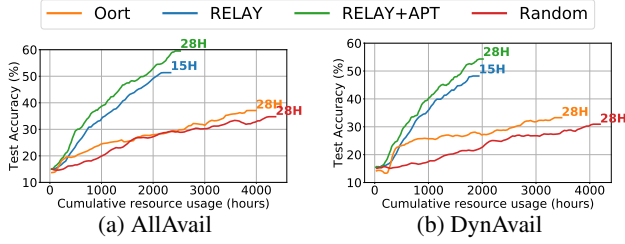


Figure 8: Training performance with Adaptive Participant Target using 50 participants in OC and different availability.

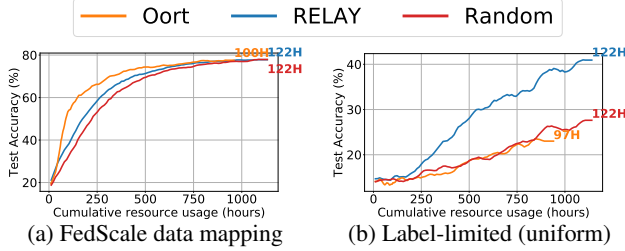


Figure 9: Performance comparison of *RELAY* vs Oort vs Random in experimental settings OC+AllAvail.

the resource consumption of *RELAY* can be further reduced with APT. Compared to AllAvail, the gains are maintained in DynAvail when *RELAY* prioritizes the least available clients and comparable accuracy is achieved. However, depending on benchmark, APT may yield no benefits when the target number of participants is small (e.g., $N_0 \leq 10$).

Stale Aggregation: We experiment with *RELAY*, Oort, and Random methods in OC+AllAvail setting. Fig. 9 shows the achieved test accuracy vs training rounds. We observe that, over different data mappings, *RELAY* can achieve good model quality with lower resource usage thanks to the SAA module. Notably, the benefits are more profound for non-IID distributions. In non-IID settings, the stale updates of delayed participants are more important compared to IID settings. This demonstrates that stale updates can boost the statistical efficiency of training. Also, *RELAY* achieves similar run-time to Random because all learners return an availability probability of 1 and hence *RELAY*’s algorithm becomes a random selection algorithm.

Stale Weight Scaling: We use OC+DynAvail and set the deadline to 100 seconds. We evaluate the weight scaling rules of §4.2.4 and present the test accuracy results over the training rounds in Fig. 10. We observe that the proposed rule (*RELAY*) consistently outperforms the other scaling rules in all data distribution scenarios. In the IID cases (Figs. 10a and 10b), the differences among the scaling rules are few accuracy points. However, in the non-IID cases (Figs. 10c to 10e), except for *RELAY*’s rule, the scaling rules have inconsistent performance. These results show the benefits of *RELAY*’s rule for mitigating the potential negative impact of stale updates. The same observations are made for OC+AllAvail. Results for FedAvg are in §D.

Learner Availability Prediction Model: We use, Prophet,

a time-series forecasting model (Taylor & Letham, 2017) and time-series data in Stunner trace (Szabó et al., 2019).⁴ We use the trace of the month of Sept-2018 and select devices with at least 1000 samples (i.e., 137 devices). We extract the plugged and charging state to train a forecasting model for each device using the first 50% of the device’s samples. We predict the future plugged state for the remaining 50% of samples and compare it to ground truth. The results show that the models predict the future charging state with high accuracy. The values of the coefficient of determination, mean square error and mean absolute error, averaged across the devices, are 0.93, 0.01, and 0.028, respectively.

5.3 Large-scale Federated Learning

We project that future FL deployments will scale significantly to include learner devices such as sensors, IoT devices, autonomous vehicles, etc., that may not be connected to power sources and have limited computational capabilities. *RELAY* enables efficient scaling over a larger number of resources, in contrast to FL systems based on post-training selection (e.g., SAFA (Wu et al., 2021)) or that skew participant selection to fast devices (e.g., Oort (Lai et al., 2021b)). Invoking all devices for training would overwhelm the server and impose significant energy usage by learners much of which would be wasted. We show the impact of large populations on resource usage using the Google speech benchmark with $3 \times$ the number of learners (3000) as earlier experiments (1000). As shown in Fig. 11, we observe that SAFA wastes many resources in the IID (Fig. 11a) and even more in the non-IID (Fig. 11b) setting.

5.4 Future Hardware Advancements

We project that the computational capability of learner devices will continue to improve and so FL systems should benefit from this. However, schemes such as Oort that favor faster learners are likely to see increased underrepresentation of low-capability learners, resulting in models that do not generalize well over a large population. In contrast, *RELAY* copes with hardware advancements by benefiting from faster learners without overlooking low-capability learners. We run the Google Speech benchmark in 4 settings using: 1) current device configurations (*HS1*); 2) device configurations with completion times (i.e., computation and communication) doubled for the top X percentile of devices (where the X is 25% (*HS2*), 75% (*HS3*) and 100% (*HS4*)). As shown in Figs. 12a and 12b, we observe both Oort and *RELAY* benefit from hardware enhancements for the IID setting. However, as shown in Fig. 12c, with a more realistic label-limited mapping (non-IID), Oort’s tendency to optimize for system speed degrades training performance significantly due to missing data from slower learners. On the other hand, *RELAY* sees significant performance gains

⁴Existing efforts use mobile traces to learn user patterns (Srinivasan et al., 2014; Yang et al., 2018a; Szabó et al., 2019).

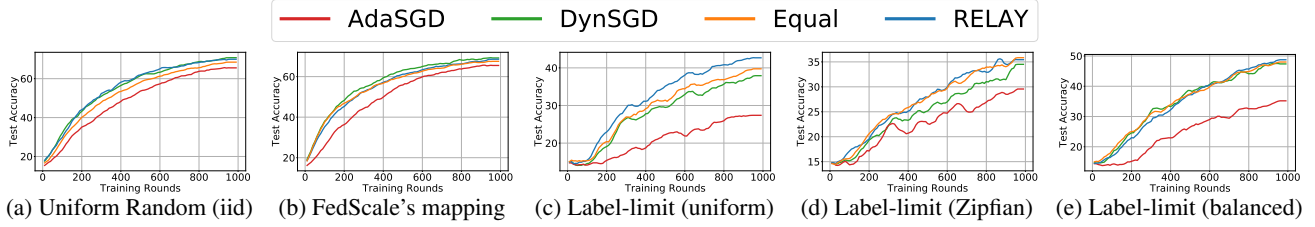


Figure 10: Performance of various scaling rules of the stale updates' weights in the aggregation step.

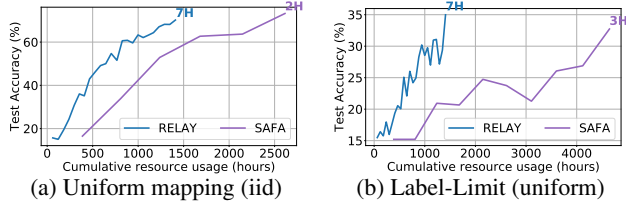


Figure 11: Resource efficiency in large-scale FL settings.

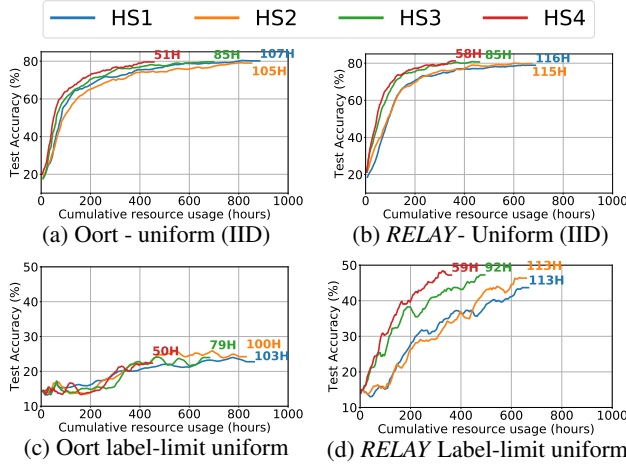


Figure 12: Impact of future hardware advancements

in the non-IID setting due to aggregation of stale updates and higher resource diversity.

6 RELATED WORK

Federated Learning (FL): A number of FL frameworks have facilitated research in this area (Caldas et al., 2018; Ryffel et al., 2018; PaddlePaddle.org, 2020; tensorflow.org, 2020; Yang et al., 2020; Lai et al., 2021a). Flash (Yang et al., 2020) extended Leaf (Caldas et al., 2018) to incorporate heterogeneity-related parameters. FedScale (Lai et al., 2021a) enables FL experimentation using a diverse set of challenging and real benchmark datasets and is the base framework we have extended in this work.

Participant Selection Strategies: A number of recent works have proposed enhanced participant selection strategies. Biasing the selection process towards learners with fast hardware and network speeds has been proposed (Nishio & Yonetani, 2018). Other work has sought to enhance statistical efficiency by selecting participants with better model

updates (Ruan et al., 2021; Chen et al., 2020). Recently, Oort (Lai et al., 2021b) proposed a strategy that combines both system and statistical efficiency. As we demonstrate in this work, these approaches either result in wasted computation or low coverage of the participant population.

Heterogeneity in FL: A significant challenge facing wider adoption of FL systems at scale is uncertainties in system behavior due to learner, system, and data heterogeneity. Learners' computational capacity can restrict contributions and extend round duration (Jiang et al., 2017; Chen et al., 2018; Abdelmoniem et al., 2021b). Architectural and algorithmic solutions to tackle heterogeneity have been proposed (Recht et al., 2011; Ho et al., 2013; Chen et al., 2016; Patarasuk & Yuan, 2009; Jiang et al., 2017; Chen et al., 2018; Abdelmoniem & Canini, 2021a). Heterogeneity in FL is particularly challenging because participants have varying data distributions and availability, as well as heterogeneous system configurations that cannot be controlled (Yang et al., 2018b; Bonawitz et al., 2019; Kairouz et al., 2019).

FL proposals: Broader improvements in FL systems have included reducing communication costs (Konečný et al., 2016; Smith et al., 2017; Bonawitz et al., 2019; Chen et al., 2019; Reisizadeh et al., 2020), improving privacy guarantees (McMahan et al., 2018; Melis et al., 2019; Bonawitz et al., 2019; Nasr et al., 2019; Bagdasaryan et al., 2020), minimizing energy consumption on edge devices (Li et al., 2019), and personalizing global models trained by participants (Jiang et al., 2019b). Recent works have sought to address the challenge of data heterogeneity (Mohri et al., 2019; Li et al., 2020b;a).

7 CONCLUSION

We studied key issues preventing the wider adoption of FL systems. We identify resource wastage and low diversity as unresolved issues in existing solutions. Therefore, taking inspiration across different aspects of existing schemes, we proposed *RELAY* that addresses these issues. *RELAY* consists of two core modules that encompass novel selection and aggregation algorithms. Compared to existing systems, *RELAY* is shown theoretically and empirically to improve model quality while reducing the amount of resources with minimal impact on training time. *RELAY* establishes an ecosystem for resource-efficient federated learning.

REFERENCES

- Abdelmoniem, A. M. and Canini, M. Towards mitigating device heterogeneity in federated learning via adaptive model quantization. In *1st Workshop on Machine Learning and Systems (EuroMLSys)*, 2021a.
- Abdelmoniem, A. M. and Canini, M. DC2: Delay-aware Compression Control for Distributed Machine Learning. In *IEEE INFOCOM*, 2021b.
- Abdelmoniem, A. M., Elzanaty, A., Alouini, M.-S., and Canini, M. An Efficient Statistical-based Gradient Compression Technique for Distributed Training Systems. In *MLSys*, 2021a.
- Abdelmoniem, A. M., Ho, C.-Y., Papageorgiou, P., Bilal, M., and Canini, M. On the Impact of Device and Behavioral Heterogeneity in Federated Learning. *arXiv 2102.07500*, 2021b.
- Bagdasaryan, E., Veit, A., Hua, Y., Estrin, D., and Shmatikov, V. How To Backdoor Federated Learning. In *AISTATS*, 2020.
- Benchmark, A. Performance ranking, 2021. URL <https://ai-benchmark.com/ranking.html>.
- Bonawitz, K., Ivanov, V., Kreuter, B., Marcedone, A., McMahan, H. B., Patel, S., Ramage, D., Segal, A., and Seth, K. Practical Secure Aggregation for Privacy-Preserving Machine Learning. In *CCS*, 2017.
- Bonawitz, K., Eichner, H., Grieskamp, W., Huba, D., Ingerman, A., Ivanov, V., Kiddon, C., Konečný, J., Mazzocchi, S., McMahan, H. B., Overveldt, T. V., Petrou, D., Ramage, D., and Roselander, J. Towards Federated Learning at Scale: System Design. In *MLSys*, 2019.
- Bonawitz, K., Salehi, F., Konečný, J., McMahan, B., and Gruteser, M. Federated learning with autotuned communication-efficient secure aggregation. In *53rd Asilomar Conference on Signals, Systems, and Computers*, pp. 1222–1226, 2019.
- Caldas, S., Duddu, S. M. K., Wu, P., Li, T., Konečný, J., McMahan, H. B., Smith, V., and Talwalkar, A. Leaf: A benchmark for federated settings. *arXiv 1812.01097*, 2018.
- Chen, C.-Y., Choi, J., Brand, D., Agrawal, A., Zhang, W., and Gopalakrishnan, K. AdaComp : Adaptive Residual Gradient Compression for Data-Parallel Distributed Training. In *AAAI*, 2018.
- Chen, J., Monga, R., Bengio, S., and Jozefowicz, R. Revisiting Distributed Synchronous SGD. In *ICLR Workshop Track*, 2016.
- Chen, W., Horvath, S., and Richtarik, P. Optimal Client Sampling for Federated Learning. *arXiv 2010.13723*, 2020.
- Chen, Y., Sun, X., and Jin, Y. Communication-efficient federated deep learning with layerwise asynchronous model update and temporally weighted aggregation. *IEEE TNNLS*, 2019.
- Damaskinos, G., Guerraoui, R., Kermarrec, A.-M., Nitu, V., Patra, R., and Taiani, F. FLeet: Online Federated Learning via Staleness Awareness and Performance Prediction. In *ACM Middleware*, 2020.
- Docs, P. Xmlrpc server and client modules, 2020. URL <https://docs.python.org/3/library/xmlrpc.html>.
- FaceBook. High-speed library for applying differential privacy for pytorch, 2021. URL <https://github.com/pytorch/opacus>.
- FedAI. Federated AI Technology Enabler, 2021. URL <https://www.fedai.org>.
- Hartmann, F., Suh, S., Komarzewski, A., Smith, T. D., and Segall, I. Federated Learning for Ranking Browser History Suggestions. *ArXiv 1911.11807*, 2019.
- He, K., Zhang, X., Ren, S., and Sun, J. Deep residual learning for image recognition. In *IEEE CVPR*, 2016.
- Ho, Q., Cipar, J., Cui, H., Kim, J. K., Lee, S., Gibbons, P. B., Gibson, G. A., Ganger, G. R., and Xing, E. P. More Effective Distributed ML via a Stale Synchronous Parallel Parameter Server. In *NeurIPS*, 2013.
- Hsu, T., Qi, H., and Brown, M. Federated Visual Classification with Real-World Data Distribution. In *ECCV*, 2020.
- Huang, J., Hong, C., Chen, L. Y., and Roos, S. Is Shapley Value fair? Improving Client Selection for Mavericks in Federated Learning. *arXiv 2106.10734*, 2021.
- Jiang, J., Cui, B., Zhang, C., and Yu, L. Heterogeneity-Aware Distributed Parameter Servers. In *SIGMOD*, 2017.
- Jiang, J., Zhou, Y., Ananthanarayanan, G., Shu, Y., and Chien, A. A. Networked Cameras Are the New Big Data Clusters. In *Proceedings of the ACM Workshop on Hot Topics in Video Analytics and Intelligent Edges (HotEdgeVideo)*, 2019a.
- Jiang, Y., Konečný, J., Rush, K., and Kannan, S. Improving federated learning personalization via model agnostic meta learning. *arXiv 1909.12488*, 2019b.

- Kairouz, P., McMahan, H. B., Avent, B., Bellet, A., Bennis, M., Bhagoji, A. N., Bonawitz, K., Charles, Z., Cormode, G., Cummings, R., et al. Advances and Open Problems in Federated Learning. *arXiv 1912.04977*, 2019.
- Konečný, J., McMahan, H. B., Yu, F. X., Richtarik, P., Suresh, A. T., and Bacon, D. Federated Learning: Strategies for Improving Communication Efficiency. In *Workshop on Private Multi-Party Machine Learning - NeurIPS*, 2016.
- Krizhevsky, A. Learning multiple layers of features from tiny images. Technical report, University of Toronto, 2009.
- Kuznetsova, A., Rom, H., Alldrin, N., Uijlings, J., Krasin, I., Pont-Tuset, J., Kamali, S., Popov, S., Mallocci, M., Kolesnikov, A., and et al. The open images dataset v4. *International Journal of Computer Vision*, 128(7): 1956–1981, 2020.
- Lai, F., Dai, Y., Zhu, X., and Chowdhury, M. FedScale: Benchmarking Model and System Performance of Federated Learning. *arXiv 2105.11367*, 2021a.
- Lai, F., Zhu, X., Madhyastha, H. V., and Chowdhury, M. Efficient Federated Learning via Guided Participant Selection. In *USENIX OSDI*, 2021b.
- Lan, Z., Chen, M., Goodman, S., Gimpel, K., Sharma, P., and Soricut, R. Albert: A lite bert for self-supervised learning of language representations. *arXiv 1909.11942*, 2020.
- Li, L., Xiong, H., Guo, Z., Wang, J., and Xu, C. Smartpc: Hierarchical pace control in real-time federated learning system. In *RTSS*, 2019.
- Li, Q., Diao, Y., Chen, Q., and He, B. Federated Learning on Non-IID Data Silos: An Experimental Study. *arXiv 2102.02079*, 2021.
- Li, T., Sahu, A. K., Zaheer, M., Sanjabi, M., Talwalkar, A., and Smith, V. Federated optimization in heterogeneous networks. In *MLSys*, 2020a.
- Li, T., Sanjabi, M., Beirami, A., and Smith, V. Fair resource allocation in federated learning. In *ICLR*, 2020b.
- Li, W., Milletari, F., Xu, D., Rieke, N., Hancox, J., Zhu, W., Baust, M., Cheng, Y., Ourselin, S., Cardoso, M. J., and Feng, A. Privacy-Preserving Federated Brain Tumour Segmentation. In *Machine Learning in Medical Imaging*, 2019.
- M-Lab. MobiPerf: an open source application for measuring network performance on mobile platforms, 2021. URL <https://www.measurementlab.net/tests/mobiperf/>.
- McMahan, B., Ramage, D., Talwar, K., and Zhang, L. Learning Differentially Private Recurrent Language Models. In *ICLR*, 2018.
- McMahan, H. B., Moore, E., Ramage, D., Hampson, S., and y Arcas, B. A. Communication-efficient learning of deep networks from decentralized data. In *AISTATS*, 2017.
- Melis, L., Song, C., De Cristofaro, E., and Shmatikov, V. Exploiting unintended feature leakage in collaborative learning. In *IEEE Symposium on Security and Privacy (SP)*, 2019.
- Mohri, M., Sivek, G., and Suresh, A. T. Agnostic federated learning. In *ICML*, 2019.
- Nasr, M., Shokri, R., and Houmansadr, A. Comprehensive privacy analysis of deep learning: Passive and active white-box inference attacks against centralized and federated learning. In *IEEE Symposium on Security and Privacy (SP)*, 2019.
- Nishio, T. and Yonetani, R. Client Selection for Federated Learning with Heterogeneous Resources in Mobile Edge. *ArXiv 1804.08333*, 2018.
- OpenMined. Syft + grid provides secure and private deep learning in python, 2020. URL <https://github.com/OpenMined/PySyft>.
- PaddlePaddle.org. Parallel distributed deep learning: Machine learning framework from industrial practice, 2020. URL <https://github.com/PaddlePaddle/PaddleFL>.
- Patarasuk, P. and Yuan, X. Bandwidth optimal all-reduce algorithms for clusters of workstations. *Journal of Parallel and Distributed Computing*, 69(2):117 – 124, 2009. ISSN 0743-7315. doi: <https://doi.org/10.1016/j.jpdc.2008.09.002>. URL <http://www.sciencedirect.com/science/article/pii/S0743731508001767>.
- Pushshift. Reddit datasets, 2020. URL <https://files.pushshift.io/reddit/>.
- Ramaswamy, S., Thakkar, O., Mathews, R., Andrew, G., McMahan, H. B., and Beaufays, F. Training Production Language Models without Memorizing User Data. *arXiv 2009.10031*, 2020.
- Recht, B., Re, C., Wright, S., and Niu, F. Hogwild: A Lock-Free Approach to Parallelizing Stochastic Gradient Descent. In *NeurIPS*, 2011.
- Reisizadeh, A., Mokhtari, A., Hassani, H., Jadbabaie, A., and Pedarsani, R. FedPAQ: A Communication-Efficient Federated Learning Method with Periodic Averaging and Quantization. In *AISTATS*, 2020.

- Ruan, Y., Zhang, X., Liang, S.-C., and Joe-Wong, C. Towards Flexible Device Participation in Federated Learning. In *AISTATS*, 2021.
- Ryffel, T., Trask, A., Dahl, M., Wagner, B., Mancuso, J., Rueckert, D., and Passerat-Palmbach, J. A generic framework for privacy preserving deep learning. *arXiv 1811.04017*, 2018.
- Smith, V., Chiang, C.-K., Sanjabi, M., and Talwalkar, A. S. Federated Multi-Task Learning. In *NeurIPS*. 2017.
- Srinivasan, V., Moghaddam, S., Mukherji, A., Rachuri, K. K., Xu, C., and Tapia, E. M. Mobileminer: Mining your frequent patterns on your phone. In *ACM UbiComp*, 2014.
- Stich, S. U. and Karimireddy, S. P. The error-feedback framework: Better rates for sgd with delayed gradients and compressed communication. *Journal of Machine Learning Research*, 2020.
- Szabó, Z., Téglás, K., Berta, A., Jelasity, M., and Bilicki, V. Stunner: A Smart Phone Trace for Developing Decentralized Edge Systems. In *19th International Conference on Distributed Applications and Interoperable Systems (DAIS)*, 2019.
- Taylor, S. J. and Letham, B. Forecasting at scale. *PeerJ Preprints 5:e3190v2*, 2017.
- Team, A. D. P. Learning with privacy at scale. *Apple Machine Learning Journal*, 2017.
- tensorflow.org. Tensorflow federated: Machine learning on decentralized data, 2020. URL <https://www.tensorflow.org/federated>.
- Wang, J. and Joshi, G. Adaptive Communication Strategies to Achieve the Best Error-Runtime Trade-off in Local-Update SGD. In *MLSys*, 2019.
- Warden, P. Speech Commands: A Dataset for Limited-Vocabulary Speech Recognition. *ArXiv 1804.03209*, 2018.
- Wu, W., He, L., Lin, W., Mao, R., Maple, C., and Jarvis, S. SAFA: A Semi-Asynchronous Protocol for Fast Federated Learning With Low Overhead. *IEEE Transactions on Computers*, 70(5), 2021.
- Xie, C., Koyejo, S., and Gupta, I. Asynchronous Federated Optimization. *arXiv 1903.03934*, 2019.
- Yan, F. Y., Ayers, H., Zhu, C., Fouladi, S., Hong, J., Zhang, K., Levis, P., and Winstein, K. Learning in situ: a randomized experiment in video streaming . In *USENIX NSDI*, 2020.
- Yang, C., Shi, X., Jie, L., and Han, J. I know you’ll be back: Interpretable new user clustering and churn prediction on a mobile social application. In *KDD*, 2018a.
- Yang, C., Wang, Q., Xu, M., Wang, S., Bian, K., and Liu, X. Heterogeneity-aware federated learning. *arXiv 2006.06983*, 2020.
- Yang, T., Andrew, G., Eichner, H., Sun, H., Li, W., Kong, N., Ramage, D., and Beaufays, F. Applied Federated Learning: Improving Google Keyboard Query Suggestions. *arXiv 1812.02903*, 2018b.
- Zhang, W., Gupta, S., Lian, X., and Liu, J. Staleness-Aware Async-SGD for Distributed Deep Learning. In *IJCAI*, 2016.
- Zhang, X., Zhou, X., Lin, M., and Sun, J. ShuffleNet: An Extremely Efficient Convolutional Neural Network for Mobile Devices. In *IEEE CVPR*, 2018.

A IMPLEMENTATION DETAILS

The design of *RELAY* is lightweight and can operate as an online service or a plug-in module to existing FL frameworks. Therefore, *RELAY* suits large-scale FL deployments dealing with likely thousands to millions of end-devices.

In each round t , during the selection phase, *RELAY* selects the participants as follows:

1. First, the server updates its estimate of the round duration μ_t and send an estimate of the future time slot $a = (\mu_t, 2\mu_t)$ to the learners during which the next round would run.
2. The learners maintain trace of their charging events and use it to periodically train a forecasting model of their future availability (i.e., charging or plugged state) which is then used to predict the future availability whenever the server inquires about the availability probability of future time-slots.
3. Upon receiving the time-slot a from the server, each the learner l uses the prediction model to infer the probability for its future availability in that time slot p_l and send it to the server.
4. The server having collected the probabilities P_t of the learners, it selects the participants using Algorithm 1.

In each round t , during the reporting phase, *RELAY* handles the stale updates as follows:

1. The server collects the stale updates similar to the fresh updates which are received before the end of current training round t .
2. Upon the end of round and during aggregation, the server aggregates the fresh updates first to produce $\hat{u}_{\mathcal{F}}$.
3. Then for each stale update u_s , compared to the timestamp of current round, the server computes the level of staleness τ_t using the timestamp of the stale update $\hat{u}_{\mathcal{F}}$ participated.
4. Then, for each stale, the server computes the deviation of the stale update from the fresh ones Λ_t and then use the proposed rule in Eq. (2) to assign the scaling weight of the stale update.
5. Then, the server aggregates the scaled stale updates with the aggregated fresh ones to produce the new model using Algorithm 2.

RELAY is implemented as a Python library on top of the FedScale framework (Lai et al., 2021a). We introduce minimal code modifications to implement the SAA and IPS module discussed in §4. We provide a simple interface to allow for the integration of both modules into the server aggregation logic and participant selection procedures, respectively. FL developers can easily integrate *RELAY*'s modules with the server program. *RELAY* can also be incorporated with FL platforms such as TensorFlow Federated (tensorflow.org, 2020) or PySyft (OpenMined, 2020)).

For instance, to integrate *RELAY* with PySyft, *RELAY* requires minimal exchange between the server and learners at the selection stage. For each learner that checks in with the server, the server need to send the learner, the estimated future time slot of the next training round to the learner. The learner uses its locally trained prediction model to produce an availability probability (i.e., a floating-point value) and send it to the server. The learners therefore do not need to exchange any sensitive information about their data rather it sends only the availability probability in the future (which may not be 100% accurate) to the server. To achieve this goal, the FL developer needs to program the FL application to send this information to the FL server at the selection stage. Notably, the size of this information is minuscule and introduces minimal memory footprint or communication overhead. *RELAY* can also run as a distributed service. In such a case, libraries such as the XML-RPC library (Docs, 2020) could be used to establish the communication channel between *RELAY* and the server. The server can share the meta-data from the participants with the *RELAY* service. The server can use PySyft API `model.send(participant_id)` to invoke the participant selected by *RELAY*, and `model.get(participant_id)` to collect the model and meta-data updates from the participant.

B CONVERGENCE ANALYSIS

Notations. In this paper, by $[d]$ we denote the set of d natural numbers $\{1, 2, \dots, d\}$. We denote the ℓ_2 norm of a vector $x \in \mathbb{R}^d$ by $\|x\|$. In the proofs, we use the notation $\mathbb{E}_t[\cdot]$ to denote expectation conditioned on the iterate x_t , that is, $\mathbb{E}[\cdot|x_t]$.

B.1 Overview of results

In §B.2, we provide the technical lemmas and inequalities necessary for the analysis. The analysis is in §B.3, with key results being Lemma 7 and Theorem 1.

B.2 Technical lemmas

Lemma 1. *If $a, b \in \mathbb{R}^d$ then the Young's inequality is: For all $\rho > 0$, we have*

$$\|a + b\|^2 \leq (1 + \rho)\|a\|^2 + (1 + \rho^{-1})\|b\|^2. \quad (3)$$

Alternatively,

$$2 \langle a, b \rangle \leq \rho\|a\|^2 + \rho^{-1}\|b\|^2. \quad (4)$$

Lemma 2. For $a_i \in \mathbb{R}^d$ we have:

$$\left\| \frac{1}{n} \sum_{i=1}^n a_i \right\|^2 \leq \frac{1}{n} \sum_{i=1}^n \|a_i\|^2. \quad (5)$$

Lemma 3. Let $r_0 \geq 0$, $c > 0$, $b \geq 0$, $d > 0$, $T > 0$, $K > 0$ and $0 < \gamma \leq \frac{1}{d}$. Then, it holds

$$\frac{r_0}{\gamma TK} + c\gamma + b\gamma^2 \leq \frac{dr_0}{TK} + \frac{2\sqrt{cr_0}}{\sqrt{TK}} + \frac{br_0}{cTK}.$$

Proof. We consider two cases. If $\frac{r_0}{cTK} \leq \frac{1}{d^2}$, then choosing the step-size $\gamma = \left(\frac{r_0}{cTK}\right)^{1/2}$, we get

$$\frac{r_0}{\gamma TK} + c\gamma + b\gamma^2 \leq \frac{2\sqrt{cr_0}}{\sqrt{TK}} + \frac{br_0}{cTK}.$$

Else, if $\frac{r_0}{cTK} > \frac{1}{d^2}$, then choosing $\gamma = \frac{1}{d}$, we get

$$\frac{r_0}{\gamma TK} + c\gamma + b\gamma^2 \leq \frac{dr_0}{TK} + \frac{c}{d} + \frac{b}{d^2} \leq \frac{dr_0}{TK} + \frac{\sqrt{cr_0}}{\sqrt{TK}} + \frac{br_0}{cTK}.$$

Combining both bounds, we get the result. \square

B.3 Perturbed iterate analysis

We first define the update of Stale-Synchronous FedAvg:

$$v_t = \begin{cases} 0, & \text{if } t < \alpha \\ \frac{1}{n} \sum_{i=1}^n \sum_{k=0}^{K-1} g_{t-\alpha, k}^i, & \text{otherwise.} \end{cases} \quad (6)$$

Using this definition of v_t , we have

$$x_{t+1} = x_t - v_t \quad \forall t. \quad (7)$$

Let us also define the *error* e_t due to asynchrony as

$$e_t = \sum_{j=1}^{\alpha} \mathbb{1}_{(t-j) \geq 0} \left(\frac{\gamma}{n} \sum_{i=1}^n \sum_{k=1}^K g_{t-j, k}^i \right). \quad (8)$$

where $\mathbb{1}_Z$ denotes the indicator function of the set Z .

The recurrence relation in the next lemma is instrumental for perturbed iterate analysis of Algorithm 2.

Lemma 4. Define the sequence of iterates $\{\tilde{x}_t\}_{t \geq 0}$ as $\tilde{x}_t = x_t - \bar{e}_t$, with $\tilde{x}_0 = x_0$. Then $\{\tilde{x}_t\}_{t \geq 0}$ satisfy the recurrence:
 $\tilde{x}_{t+1} = \tilde{x}_t - \frac{\gamma}{n} \sum_{i=1}^n \sum_{k=0}^{K-1} g_{t, k}^i.$

Proof. We have

$$\begin{aligned} \tilde{x}_{t+1} &= x_{t+1} - e_{t+1} = x_t - \mathbb{1}_{(t-\alpha) \geq 0} \left(\frac{\gamma}{n} \sum_{i=1}^n \sum_{k=1}^K g_{t-j, k}^i \right) - \left(e_t + \frac{\gamma}{n} \sum_{i=1}^n \sum_{k=1}^K g_{t, k}^i - \mathbb{1}_{(t-\alpha) \geq 0} \left(\frac{\gamma}{n} \sum_{i=1}^n \sum_{k=1}^K g_{t-j, k}^i \right) \right) \\ &= \tilde{x}_t - \frac{\gamma}{n} \sum_{i=1}^n \sum_{k=0}^{K-1} g_{t, k}^i. \end{aligned}$$

Hence the result. \square

Lemmas 5 and 6 are useful for bounding intermediate terms in the analysis.

Lemma 5. We have

$$\mathbb{E}_t \left\| \frac{1}{n} \sum_{i=1}^n \sum_{k=0}^{K-1} g_{t, k}^i \right\|^2 \leq \frac{1}{n} \sum_{i=1}^n \sum_{k=0}^{K-1} (K + \frac{M}{n}) \|\nabla f(y_{t, k}^i)\|^2 + \frac{K\sigma^2}{n}. \quad (9)$$

Proof. We have

$$\begin{aligned}
 \mathbb{E}_t \left\| \frac{1}{n} \sum_{i=1}^n \sum_{k=0}^{K-1} g_{t,k}^i \right\|^2 &= \mathbb{E}_t \left\| \frac{1}{n} \sum_{i=1}^n \sum_{k=0}^{K-1} (\nabla f(y_{t,k}^i) + \xi_{t,k}^i) \right\|^2 \\
 &\stackrel{\mathbb{E}[\xi_{t,k}^i | x_t]=0}{=} \mathbb{E}_t \left\| \frac{1}{n} \sum_{i=1}^n \sum_{k=0}^{K-1} \nabla f(y_{t,k}^i) \right\|^2 + \mathbb{E}_t \left\| \frac{1}{n} \sum_{i=1}^n \sum_{k=0}^{K-1} \xi_{t,k}^i \right\|^2 \\
 &\stackrel{\mathbb{E}[\xi_{t,k}^i | x_t]=0}{=} \mathbb{E}_t \left\| \frac{1}{n} \sum_{i=1}^n \sum_{k=0}^{K-1} \nabla f(y_{t,k}^i) \right\|^2 + \frac{1}{n^2} \sum_{i=1}^n \sum_{k=0}^{K-1} \mathbb{E}_t \|\xi_{t,k}^i\|^2 \\
 &\stackrel{\text{By Assumption 3}}{\leq} \mathbb{E}_t \left\| \frac{1}{n} \sum_{i=1}^n \sum_{k=0}^{K-1} \nabla f(y_{t,k}^i) \right\|^2 + \frac{1}{n^2} \sum_{i=1}^n \sum_{k=0}^{K-1} (M \|\nabla f(y_{t,k}^i)\|^2 + \sigma^2) \\
 &\stackrel{(3)}{\leq} \frac{K}{n} \sum_{i=1}^n \sum_{k=0}^{K-1} \|\nabla f(y_{t,k}^i)\|^2 + \frac{1}{n^2} \sum_{i=1}^n \sum_{k=0}^{K-1} M \|\nabla f(y_{t,k}^i)\|^2 + \frac{K\sigma^2}{n}
 \end{aligned}$$

By rearranging the terms we get the result. \square

Lemma 6. With a constant step-size $\gamma \leq \frac{1}{2L\sqrt{\alpha K(n\alpha K + M)}}$, we have

$$\sum_{t=0}^{T-1} \frac{1}{n} \sum_{i=1}^n \sum_{k=0}^{K-1} \mathbb{E} \|\tilde{x}_t - y_{t,k}^i\|^2 \leq \frac{1}{4L^2} \sum_{t=0}^{T-1} \frac{1}{n} \sum_{i=1}^n \sum_{k=0}^{K-1} \mathbb{E} \|\nabla f(y_{t,k}^i)\|^2 + \frac{\gamma^2}{n} T \alpha K^2 \sigma^2. \quad (10)$$

Proof. In this proof, for a light notation, we will sum only over positive round indices, without writing the indicator function.

$$\begin{aligned}
 \mathbb{E} \|\tilde{x}_t - y_{t,k}^i\|^2 &= \mathbb{E} \|\tilde{x}_t - x_t + x_t - y_{t,k}^i\|^2 = \mathbb{E} \left\| \frac{\gamma}{n} \sum_{j=1}^{\alpha} \sum_{i=1}^n \sum_{k=0}^{K-1} g_{t-j,k}^i - \frac{\gamma}{n} \sum_{i=1}^n \sum_{l=0}^{k-1} g_{t,k}^i \right\|^2 \\
 &\leq \frac{\gamma^2}{n^2} (n\alpha K + M) \sum_{j=1}^{\alpha} \sum_{i=1}^n \sum_{k=0}^{K-1} \mathbb{E} \|\nabla f(y_{t-j,k}^i)\|^2 + \frac{\gamma^2}{n} \alpha K \sigma^2.
 \end{aligned}$$

Using this, we have

$$\begin{aligned}
 \sum_{t=0}^{T-1} \frac{1}{n} \sum_{i=1}^n \sum_{k=0}^{K-1} \mathbb{E} \|\tilde{x}_t - y_{t,k}^i\|^2 &\leq \frac{\gamma^2}{n^2} (K(n\alpha K + M)) \sum_{t=0}^{T-1} \sum_{j=1}^{\alpha} \sum_{i=1}^n \sum_{k=0}^{K-1} \mathbb{E} \|\nabla f(y_{t-j,k}^i)\|^2 + \frac{\gamma^2}{n} T \alpha K^2 \sigma^2 \\
 &\leq \frac{\gamma^2}{n^2} (\alpha K(n\alpha K + M)) \sum_{t=0}^{T-1} \sum_{i=1}^n \sum_{k=0}^{K-1} \mathbb{E} \|\nabla f(y_{t,k}^i)\|^2 + \frac{\gamma^2}{n} T \alpha K^2 \sigma^2 \\
 &\leq \frac{\gamma^2}{n^2} (\alpha K(n\alpha K + M)) \sum_{t=0}^{T-1} \sum_{i=1}^n \sum_{k=0}^{K-1} \mathbb{E} \|\nabla f(y_{t,k}^i)\|^2 + \frac{\gamma^2}{n} T \alpha K^2 \sigma^2 \\
 &\stackrel{\gamma \leq \frac{1}{2L}\sqrt{\frac{n}{\alpha K(n\alpha K + M)}}}{\leq} \frac{1}{4L^2} \sum_{t=0}^{T-1} \frac{1}{n} \sum_{i=1}^n \sum_{k=0}^{K-1} \mathbb{E} \|\nabla f(y_{t,k}^i)\|^2 + \frac{\gamma^2}{n} T \alpha K^2 \sigma^2.
 \end{aligned}$$

Lemma 7. Let Assumptions 1, 2 and 3 hold. If $\{x_t\}_{t \geq 0}$ denote the iterates of Algorithm 2 for a constant setp-size, $\gamma \leq \min\{\frac{1}{2L\sqrt{\alpha K(n\alpha K + M)}}, \frac{n}{2L(nK + M)}\}$, then

$$\frac{1}{nTK} \sum_{t=0}^{T-1} \sum_{i=1}^n \sum_{k=0}^{K-1} \mathbb{E} \|\nabla f(y_{t,k}^i)\|^2 \leq \frac{8}{\gamma TK} (f(x_0) - f^*) + \frac{4\gamma L\sigma^2}{n} + \frac{4\gamma^2 L^2 \alpha K \sigma^2}{n}. \quad (11)$$

Proof. By using the L -smoothness of f and taking expectation we have

$$\begin{aligned}
 \mathbb{E}_t[f(\tilde{x}_{t+1})] &\leq f(\tilde{x}_t) - \langle \nabla f(\tilde{x}_t), \mathbb{E}_t[\tilde{x}_{t+1} - \tilde{x}_t] \rangle + \frac{L}{2} \mathbb{E}_t \|\tilde{x}_{t+1} - \tilde{x}_t\|^2 \\
 &= f(\tilde{x}_t) - \left\langle \nabla f(\tilde{x}_t), \frac{\gamma}{n} \sum_{i=1}^n \sum_{k=0}^{K-1} \nabla f(y_{t,k}^i) \right\rangle + \frac{\gamma^2 L}{2} \mathbb{E}_t \left\| \frac{1}{n} \sum_{i=1}^n \sum_{k=0}^{K-1} g_{t,k}^i \right\|^2 \\
 &\stackrel{(9)}{\leq} f(\tilde{x}_t) - \frac{\gamma}{n} \sum_{i=1}^n \sum_{k=0}^{K-1} \langle \nabla f(\tilde{x}_t), \nabla f(y_{t,k}^i) \rangle \\
 &\quad + \frac{\gamma^2 L}{2} \left(\frac{1}{n} \sum_{i=1}^n \sum_{k=0}^{K-1} (K + \frac{M}{n}) \|\nabla f(y_{t,k}^i)\|^2 + \frac{K\sigma^2}{n} \right) \\
 &\leq f(\tilde{x}_t) - \frac{\gamma}{n} \sum_{i=1}^n \sum_{k=0}^{K-1} \|\nabla f(y_{t,k}^i)\|^2 + \frac{\gamma}{n} \sum_{i=1}^n \sum_{k=0}^{K-1} \langle \nabla f(y_{t,k}^i) - \nabla f(\tilde{x}_t), \nabla f(y_{t,k}^i) \rangle \\
 &\quad + \frac{\gamma^2 L}{2} \left(\frac{1}{n} \sum_{i=1}^n \sum_{k=0}^{K-1} (K + \frac{M}{n}) \|\nabla f(y_{t,k}^i)\|^2 + \frac{K\sigma^2}{n} \right) \\
 &\stackrel{(4)}{\leq} f(\tilde{x}_t) - (\gamma - \frac{\gamma}{2} - \frac{\gamma^2 L(nK + M)}{2n}) \frac{1}{n} \sum_{i=1}^n \sum_{k=0}^{K-1} \|\nabla f(y_{t,k}^i)\|^2 + \\
 &\quad \frac{\gamma}{2} \frac{1}{n} \sum_{i=1}^n \sum_{k=0}^{K-1} \|\nabla f(\tilde{x}_t) - \nabla f(y_{t,k}^i)\|^2 + \frac{\gamma^2 LK\sigma^2}{2n} \\
 &\leq f(\tilde{x}_t) - \frac{\gamma}{2} (1 - \frac{\gamma L(nK + M)}{n}) \frac{1}{n} \sum_{i=1}^n \sum_{k=0}^{K-1} \|\nabla f(y_{t,k}^i)\|^2 + \\
 &\quad \frac{\gamma}{2} \frac{1}{n} \sum_{i=1}^n \sum_{k=0}^{K-1} \|\nabla f(\tilde{x}_t) - \nabla f(y_{t,k}^i)\|^2 + \frac{\gamma^2 LK\sigma^2}{2n} \\
 &\stackrel{\gamma \leq \frac{n}{2L(nK+m)}}{\leq} f(\tilde{x}_t) - \frac{\gamma}{4} \frac{1}{n} \sum_{i=1}^n \sum_{k=0}^{K-1} \|\nabla f(y_{t,k}^i)\|^2 + \frac{\gamma}{2} \frac{1}{n} \sum_{i=1}^n \sum_{k=0}^{K-1} \|\nabla f(\tilde{x}_t) - \nabla f(y_{t,k}^i)\|^2 + \frac{\gamma^2 LK\sigma^2}{2n} \\
 &\leq f(\tilde{x}_t) - \frac{\gamma}{4} \frac{1}{n} \sum_{i=1}^n \sum_{k=0}^{K-1} \|\nabla f(y_{t,k}^i)\|^2 + \frac{\gamma}{2} \frac{1}{n} \sum_{i=1}^n \sum_{k=0}^{K-1} \|\nabla f(x_t) - \nabla f(y_{t,k}^i)\|^2 + \frac{\gamma^2 LK\sigma^2}{2n} \\
 &\stackrel{L\text{-smoothness}}{\leq} f(\tilde{x}_t) - \frac{\gamma}{4} \frac{1}{n} \sum_{i=1}^n \sum_{k=0}^{K-1} \|\nabla f(y_{t,k}^i)\|^2 + \gamma L^2 \frac{1}{2n} \sum_{i=1}^n \sum_{k=0}^{K-1} \|\tilde{x}_t - y_{t,k}^i\|^2 + \frac{\gamma^2 LK\sigma^2}{2n}
 \end{aligned}$$

Taking total expectation, summing over $t = 0$ to $t = T - 1$, we have

$$\begin{aligned}
 \mathbb{E}[f(\tilde{x}_T)] &\leq f(x_0) - \frac{\gamma}{4} \sum_{t=0}^{T-1} \frac{1}{n} \sum_{i=1}^n \sum_{k=0}^{K-1} \mathbb{E} \|\nabla f(y_{t,k}^i)\|^2 + \gamma L^2 \sum_{t=0}^{T-1} \frac{1}{2n} \sum_{i=1}^n \sum_{k=0}^{K-1} \mathbb{E} \|\tilde{x}_t - y_{t,k}^i\|^2 + \frac{\gamma^2 LTK\sigma^2}{2n} \\
 &\stackrel{(10)}{\leq} f(x_0) - \frac{\gamma}{4} \sum_{t=0}^{T-1} \frac{1}{n} \sum_{i=1}^n \sum_{k=0}^{K-1} \mathbb{E} \|\nabla f(y_{t,k}^i)\|^2 + \frac{\gamma}{8} \sum_{t=0}^{T-1} \frac{1}{n} \sum_{i=1}^n \sum_{k=0}^{K-1} \mathbb{E} \|\nabla f(y_{t,k}^i)\|^2 + \frac{\gamma^3}{2n} L^2 T \alpha K^2 \sigma^2 + \frac{\gamma^2 LTK\sigma^2}{2n} \\
 &= f(x_0) - \frac{\gamma}{8} \sum_{t=0}^{T-1} \frac{1}{n} \sum_{i=1}^n \sum_{k=0}^{K-1} \mathbb{E} \|\nabla f(y_{t,k}^i)\|^2 + \frac{\gamma^3}{2n} L^2 T \alpha K^2 \sigma^2 + \frac{\gamma^2 LTK\sigma^2}{2n}
 \end{aligned}$$

Rearranging, we get

$$\begin{aligned} \frac{1}{nTK} \sum_{t=0}^{T-1} \sum_{i=1}^n \sum_{k=0}^{K-1} \mathbb{E} \|\nabla f(y_{t,k}^i)\|^2 &\leq \frac{8}{\gamma TK} (f(x_0) - \mathbb{E}[f(\tilde{x}_T)]) + \frac{4\gamma L\sigma^2}{n} + \frac{4\gamma^2 L^2 \alpha K \sigma^2}{n} \\ &\leq \frac{8}{\gamma TK} (f(x_0) - f^*) + \frac{4\gamma L\sigma^2}{n} + \frac{4\gamma^2 L^2 \alpha K \sigma^2}{n}. \end{aligned}$$

□

B.3.1 Final convergence result

The following theorem describes the $\mathcal{O}(1/\sqrt{nTK})$ convergence of Algorithm 2 with an appropriate step-size.

Theorem. 1 Let Assumptions 1, 2, and 3 hold. Then

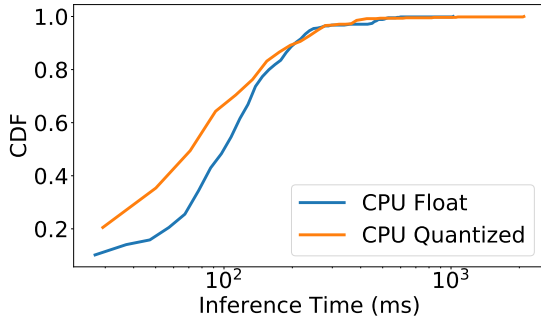
$$\frac{1}{nTK} \sum_{t=0}^{T-1} \sum_{i=1}^n \sum_{k=0}^{K-1} \mathbb{E} \|\nabla f(y_{t,k}^i)\|^2 = \mathcal{O} \left(\frac{\sigma \sqrt{L(f(x_0) - f^*)}}{\sqrt{nTK}} + \frac{\max\{L\sqrt{\alpha K(n\alpha K + M)}, L(K + M/n)\}}{TK} \right). \quad (12)$$

Proof. We invoke Lemma 3 in Lemma 7 with $r_0 = 8(f(x_0) - f^*)$, $c = \frac{4L\sigma^2}{n}$, $b = \frac{4L^2\alpha K\sigma^2}{n}$, and $d = \max\{2L\sqrt{\alpha K(n\alpha K + M)}, 2L(nK + M)/n\}$. □

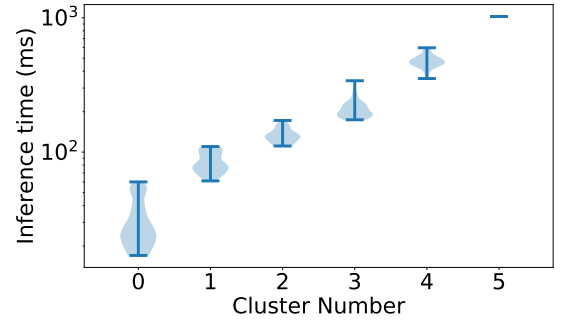
C LEARNERS' HETEROGENEITY

In this part, we discuss the heterogeneity of the learners in terms of the device heterogeneity and their availability dynamics.

Analysis of Learner Computation Speed We show the distribution and clustering of the device computational speed (or inference time) as extracted from the AI mobile benchmark (Benchmark, 2021). AI Benchmark maintains the inference speed of popular DNN models (e.g., MobileNet) on a wide range of Android-based end-devices (e.g., Samsung Galaxy S20 and Huawei P40). Fig. 13a show that the learners have high device heterogeneity among each other with long tail distribution. Fig. 13b shows that the learners could be grouped into 6 clusters of different device configurations according to their computational capabilities. This demonstrates that learners would have a highly variable completion time during the training.



(a) CDF of Inference time



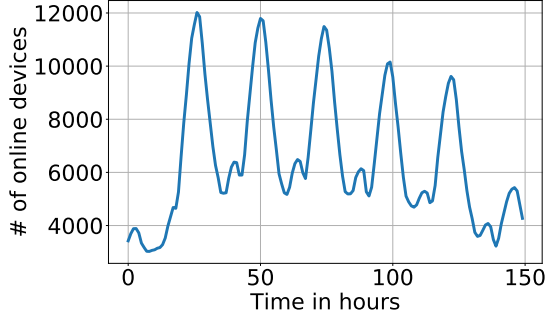
(b) Clustering of Devices based on Speed

Figure 13: Computational speeds of the end-devices. (Left) CDF of device infer. time; (Right) Clusters of device capacity

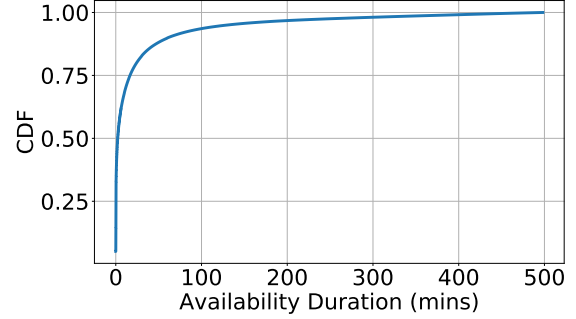
Analysis of Learners' Availability: We show the availability dynamics of the learners as extracted from the user behavior trace in (Yang et al., 2020). Fig. 14a show that the number of available learners over the time vary significantly and they exhibit a diurnal patterns over the days of the week where large number of learners are mostly available (i.e., charging) during night time. Fig. 14b shows the CDF of the length of learners' availability time-slot and it demonstrates that the availability duration of the learners have a very long tail. However, most of the clients (up to 70%) are available for less than 10 minutes.

D RESULTS

In this part, we provide more results for the other benchmarks and experimental settings and configuration to support the observations made on RELAY.



(a) dynamics of the number of available clients.



(b) CDF of the availability period

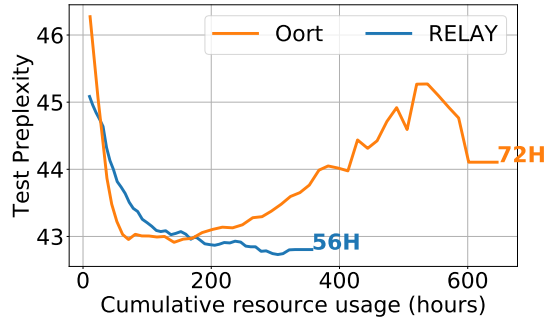
Figure 14: Analysis of availability. (Left) Availability’s diurnal pattern; (Right) CDF of learners’ availability.

D.1 Results of Other Benchmarks

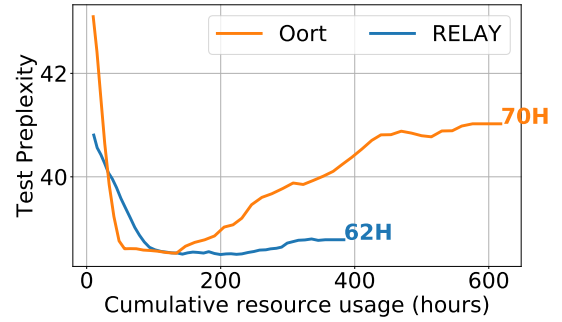
We present the comparison of *RELAY* with Oort in Natural Language Processing (NLP) and Computer Vision (CV) benchmarks.

D.2 Experiments in OC+DynAvail settings

We run OpenImage, CIFAR10, Reddit and StackOverFlow benchmarks using experimental setting **OC+DynAvail**. In this scenario, we compare the performance *RELAY* and Oort system. We use YoGi as the aggregation algorithm for Open Image, Reddit and StackOverFlow benchmarks and FedAvg for CIFAR10 benchmarks. Adaptive Participant Target (APT) were enabled for *RELAY*.



(a) Reddit - FedScale mapping



(b) Stackoverflow - FedScale mapping

Figure 15: The training performance for NLP benchmarks in OC+DynAvail setting.

Due to the large size of NLP benchmarks, we use FedScale mappings but limit the whole dataset size to 20% (i.e., ≈ 8 Million samples). Fig. 15 shows the performance results in the natural language processing tasks of the Reddit and StackOverFlow benchmarks. Again, the results show that, with considerable lower consumption of learners’ resources, *RELAY* achieves significant improvements in the test perplexity of the trained model over Oort.

Fig. 16 shows the performance results in computer vision tasks of CIFAR10 and Open Image Benchmarks. The results, over fedscale and label-limited data mappings, show that *RELAY*, with noticeable lower consumption of learners’ resources, achieves better model accuracy over Oort, especially when data is non-iid distributed. The improvements are thanks to both the IPS and SAA modules of *RELAY*. Specifically, IPS increases the rate of unique participants and SAA helps with improving the statistical efficiency of the model using stragglers’ stale contributions via stale updates aggregation.

In summary, the results over different benchmarks and scenarios demonstrate that *RELAY* results in an FL system with superior performance compared to existing state-of-the-art systems.

D.3 Experiments in OC+AllAvail settings

We repeat the previous experiments and run OpenImage, CIFAR10, Reddit and StackOverFlow benchmarks using experimental setting **OC+AllAvail**.

Due to the large size of NLP benchmarks, we use FedScale mappings but limit the whole dataset size to 20% (i.e., ≈ 8 Million samples). Fig. 17 shows the performance results in the natural language processing tasks of the Reddit and StackOverFlow benchmarks. Again, the results show that, with considerable lower consumption of learners’ resources,

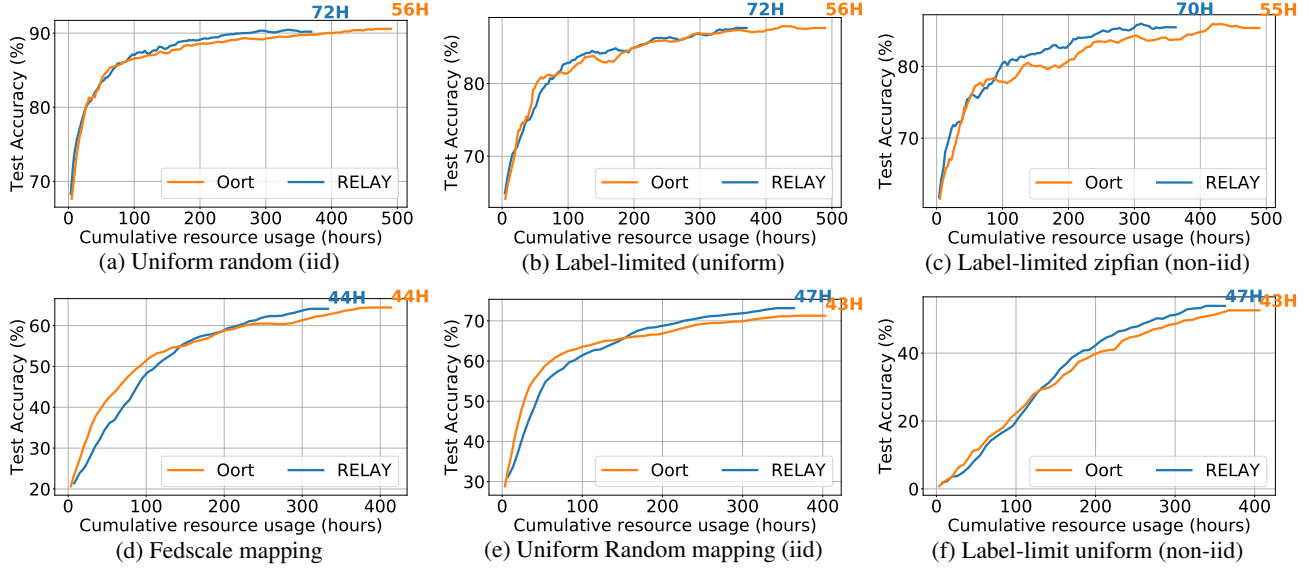


Figure 16: The training performance for CIFAR10 [(a), (b), (c)] and OpenImage [(d), (e), (f)] benchmarks in OC+DynAvail setting.

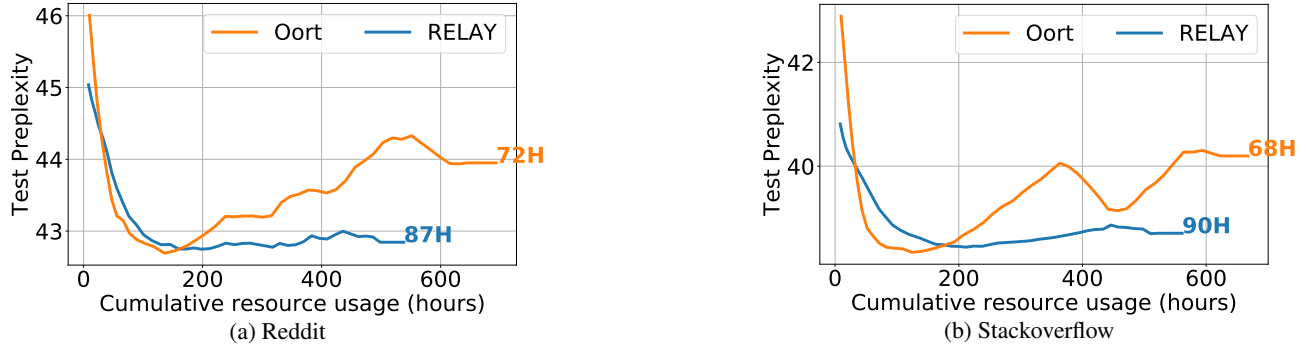


Figure 17: The training performance for NLP benchmarks in OC+AllAvail setting.

RELAY achieves significant improvements in the test perplexity of the trained model over Oort.

Fig. 18 shows the performance results in computer vision tasks of CIFAR10 and Open Image Benchmarks. The results, over fedscale and label-limited data mappings, show that *RELAY*, with noticeable lower consumption of learners' resources, achieves better model accuracy over Oort, especially when data is non-iid distributed. The improvements are thanks to the SAA module of *RELAY* since the IPS module would revert to random selection method when all clients are always available (i.e., they return availability probability value of 1). Specifically, in this scenario, SAA helps with improving the statistical efficiency of the model using stragglers' stale contributions via stale updates aggregation. In summary, even in settings where the clients are always available (e.g., cross-silo settings), the results over different benchmarks and scenarios demonstrate that *RELAY* results in an FL system with superior performance compared to existing state-of-the-art systems.

D.4 Weight Scaling with FedAvg

We use experimental settings OC+AllAvail. We use Google Speech Benchmark and FedAvg as the aggregation algorithm instead of YoGi. We set the deadline to 100s. We evaluate the weight scaling rules of §4.2.4 and present the test accuracy results over the training rounds in Fig. 19. Similar to observations made with YoGi, We find that, the rule used in *RELAY* consistently outperforms the other scaling rules over all data distributions. In the iid cases (Fig. 19a Fig. 19b), the differences among the scaling rules are few accuracy points. And again, in the non-iid cases (Figs. 19c to 19e), show that the scaling rules inconsistent performance. These results confirms that the proposed rule in *RELAY* improves the performance and is beneficial over existing rules.

D.5 Empirical Convergence Results

We run both *RELAY* and Oort for longer number of rounds and observe the accuracy they converge to (i.e., no longer the accuracy improves). Fig. 20 shows that *RELAY* can converge to a very high accuracy compared to Oort (nearly up to 20

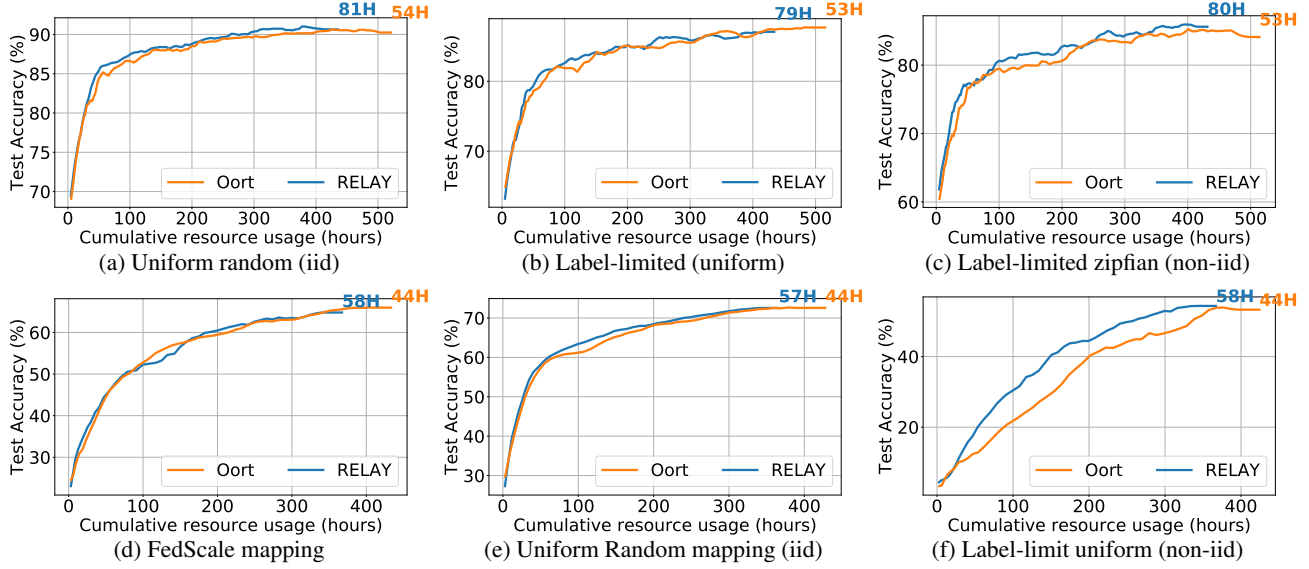


Figure 18: The training performance for CIFAR10 [(a), (b), (c)] and OpenImage [(d), (e), (f)] benchmarks in CO+AllAvail.

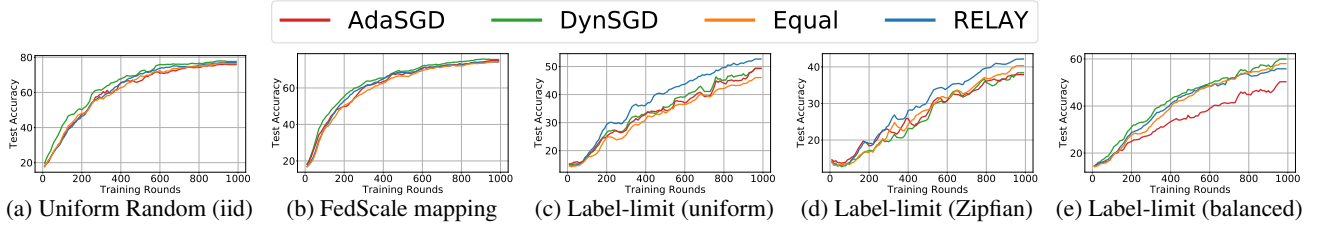


Figure 19: Performance of various scaling rules of the stale updates' weights in the aggregation step of FedAvg algorithm. *RELAY* can achieve this with both less resources and time compared to Oort. This demonstrates that even running Oort for longer rounds it can not improve or reach the same accuracy of *RELAY*.

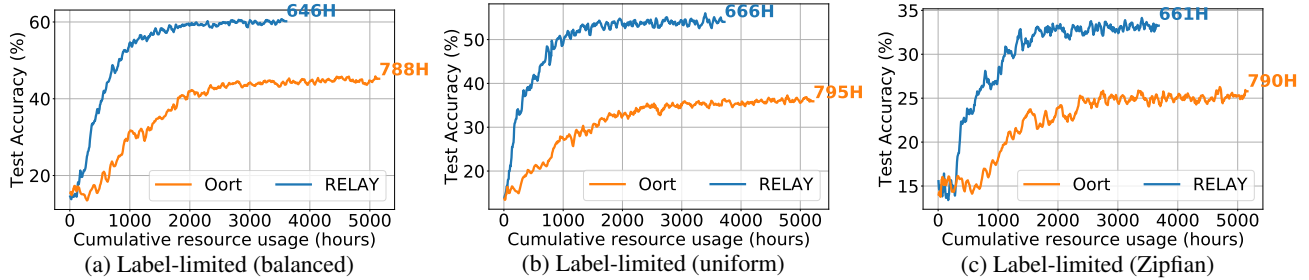


Figure 20: Training convergence comparison under OC+DynAvail across the Label-limited (non-iid) data mappings.

E DATASETS

We describe briefly the datasets used in this work which were presented by the FedScale Framework (Lai et al., 2021a).

Google Speech Commands: is a dataset for speech recognition task which consists of over ten thousands of audio clips recorded for most common words in English language (Warden, 2018). Each clip lasts for roughly a single second of time and the recorded voice of thousands of different people speaking 35 English words such as the 10 digits (0-9), Yes, No, Up, Down, etc.

CIFAR10: is a dataset for computer vision tasks which consists of 60K 32x32 colour images. The images are taken from 10 classes and the classes are distributed uniformly among the images (i.e., 6000 images per class). There are 50000 training images and 10000 test images. The dataset is divided into five training batches and one test batch, each with 10000 images. The test batch contains exactly 1000 randomly-selected images from each class. The training batches contain the remaining images in random order, but some training batches may contain more images from one class than another. Between them,

the training batches contain exactly 5000 images from each class.

OpenImage: is a dataset for computer vision task which consists of nearly 1.2 million images gathered from Flickr hosting website (Kuznetsova et al., 2020). The dataset consists of approximately 16 Million image bounding boxes for 600 different objects such as Microwave oven, fedora hat, snowman, etc. The dataset is cleaned up to match the provided indices of clients which is used for the data to client mapping. The image bounding boxes are of size 256×256 pixels.

Reddit: is a dataset consisting of user comments extracted from the Reddit website (Pushshift, 2020). This dataset is commonly used for training nlp models. Each user as a client and the dataset is restricted to the 30k most frequently used words. Hence, each sentence as is represented as a sequence of indices matching these 30k frequently used words.

StackOverflow: is similar to the reddit dataset, StackOverflow consists of the user comments extracted from the StackOverflow website (McMahan et al., 2017). Each user is also as a client and the dataset is also restricted to the 30k most frequently used words.

E.1 Analysis of Data Labels

We show the frequency of label appearance on the learners in the FedScale data mappings for the Google Speech benchmark in Fig. 21. The label frequency on the learners demonstrate that all labels appear on at least once on nearly 40% of the devices. Each label also appear up to more than 10 times on the devices. This demonstrates that, in the FedScale data mapping, the data samples of the labels are well distributed on the clients and is close to a uniform (iid) distribution.

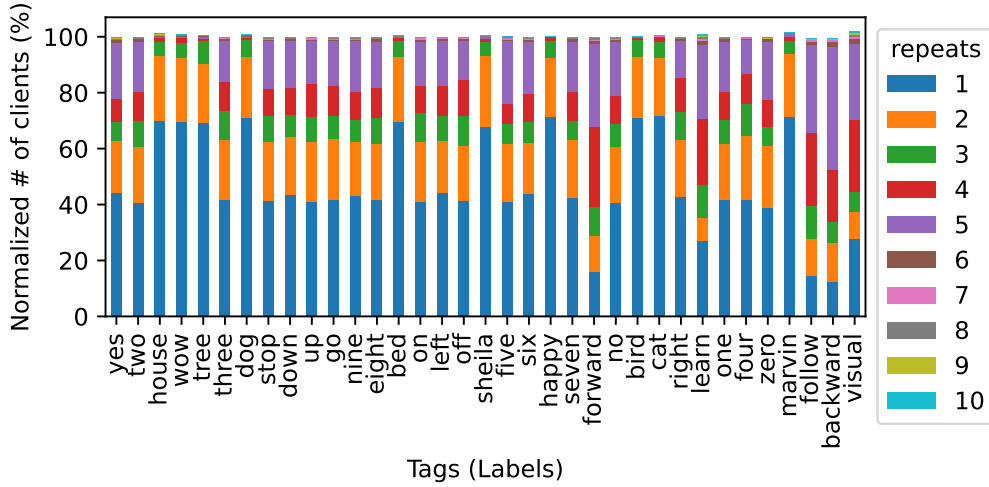


Figure 21: Number of label repetitions on the learners.

E.2 Baseline Performance in Semi-Centralized Training

We experiment with the various benchmarks in a semi-centralized setting which resembles traditional data-parallel distributed learning. We partition the full dataset among only a total of 10 learners then in each training round all learners participate fully in the distributed training process and in updating of the model. The results of the final achieved accuracy for different data mappings are presented in which constitute the baseline performance.

Table 2: Baseline Performance with Centralized Training.

Benchmark	Quality Metric	Aggregation Algorithm	Data to Learner Mapping			
			Uniform Random	Label-limited		
				Uniform Random	Zipf Distribution	Balanced
CIFAR10	Top-5 Test Accuracy	FedAvg	90.4	86.1	76.4	86.4
Open Image	Top-5 Test Accuracy	YoGi	70.7	30.6	32.3	35.5
Google Speech	Top-5 Test Accuracy	YoGi	76.5	34.7	33.4	37.1
Reddit	Test Perplexity	YoGi	43.6	N/A	N/A	N/A
Stackoverflow	Test Perplexity	YoGi	40.2	N/A	N/A	N/A